J Am Soc Nephrol 14: 981–991, 2003

Retinoids Regulate the Repairing Process of the Podocytes in Puromycin Aminonucleoside-induced Nephrotic Rats

AKIRA SUZUKI,* TAKAHITO ITO,* ENYU IMAI,* MASAYA YAMATO,* HIROTSUGU IWATANI,* HIROSHI KAWACHI,† and MASATSUGU HORI*

**Department of Internal Medicine and Therapeutics, Osaka University Graduate School of Medicine, Suita, Osaka, Japan; and †Department of Cell Biology, Institute of Nephrology, Niigata University Graduate School of Medical and Dental Sciences, Niigata, Japan.*

Abstract. The foot processes forming the slit diaphragm are disrupted in diseases associated with proteinuria. Although they are often repairable, regulators for the repairing process remain unknown. By extrapolating from the fact that vitamin A is essential for the nephrogenesis, this study examined whether or not injured podocytes in the middle of the repairing process require retinaldehyde dehydrogenase type 2 (RALDH2), one of the key enzymes to produce all-*trans*-retinoic acid (ATRA). RALDH2 was dramatically upregulated in podocytes of puromycin aminonucleoside-induced nephrosis (PAN nephrosis) rats. On day 5 of PAN nephrosis, RALDH2 showed the remarkable induction, whereas glomerular expression levels of nephrin and midkine, one of the ATRA target genes, were downregulated. Daily administration of ATRA ameliorated proteinuria, which was accompanied by the improvement in the effacement of the foot processes and by the induction of nephrin and midkine. In contrast, recovery from PAN nephrosis was delayed in rats fed with a vitamin A-deficient diet. Consistently, the promoter region of human nephrin gene (NPHS1) contained three putative retinoic acid response elements (RARE) and showed the enhancer activity in response to ATRA in a dose-dependent manner. This transcriptional activation was regulated through the receptors for retinoids because BMS-189453, an antagonist to the retinoid receptors, counteracted it in a dose-dependent manner. In conclusion, active metabolites of vitamin A, especially ATRA produced by RALDH2 play relevant roles during the repairing process of injured podocytes. The results obtained from PAN nephrosis rats might be applicable to human renal diseases.

All-*trans*-retinoic acid (ATRA), an active metabolite of vitamin A, exerts a wide variety of biologic effects such as cell proliferation, apoptosis, differentiation, reproduction, maintenance of normal tissues, especially of epithelial cells (1). ATRA is generated from vitamin A through a series of oxidation mediated by both the alcohol dehydrogenase family and the aldehyde dehydrogenase family, including retinaldehyde dehydrogenase type2 (RALDH2), the key enzyme producing ATRA (2). ATRA induces the expression of several target genes responsible for the diverse biologic effects via the cognate receptors for retinoids, which are referred to as retinoic acid receptors (RAR) and retinoid X receptors (RXR). The fact that different genes are activated by different concentration of ATRA (3,4) may account for the spacio-temporal distribution of RAR and RXR and for the wide variation of retinoic acid response elements (RARE). The RARE can be divided into three classes. The most potent response element comprises the direct repeat of the consensus sequence, AGGTCA, which is separated by one, two, three, four, or five nucleotides. The palindrome structure made of two consensus sequences is less responsive to retinoic acid than the direct repeat, and it requires overexpression of RAR to be active. Finally, the complex type, which is composed of sequences that are highly degenerated from the consensus and that scatter randomly along the promoter region, is only weakly responsive (5).

Vitamin A plays a crucial role in the nephrogenesis as well as the embryogenesis. In the 1940s, Wilson *et al.* (6) demonstrated that pregnant rats fed with a diet lacking in vitamin A showed diverse renal abnormalities such as hypoplastic or ectopic ureters, horseshoe kidney, and renal hypoplasia. Even mild vitamin A deficiency induces a reduction of the nephron number, while other organs develop in a normal way (7). Recently, it is reported that a role of vitamin A in the nephrogenesis is to regulate epithelial/mesenchymal interactions through the expression of c-ret, a receptor for glial cell line-derived neurotrophic factor (GDNF), and to induce branching of the ureteric bud (8–10). However, these facts are not sufficient to account for the various renal abnormalities observed in vitamin A-deficient animals.

The glomerular epithelial cell, also called the podocyte, arises from the metanephric blastema that also produces other nephron segments such as the proximal and distal tubules. Despite highly specialized features of the podocyte, factors regulating its differentiation process and maintaining its struc-

Received August 8, 2002. Accepted January 6, 2003.

Correspondence to Dr. Takahito Ito, Department of Internal Medicine and Therapeutics, Osaka University School of Medicine, A8, 2-2 Yamadaoka, Suita, Osaka 565-0871, Japan. Phone: 81-6-6879-3632; Fax: 81-6-6879-3639; E-mail: taka@medone.med.osaka-u.ac.jp

1046-6673/1404-0981
Journal of the American Society of Nephrology

DOI: 10.1097/01.ASN.0000057857.66268.8F

tural integrity after the terminal differentiation remains unknown. Effacement of foot processes, which is associated with proteinuria in many renal diseases, is reparable when therapeutic approaches are successfully employed. However, regulators for this regeneration process are also unknown.

In this study, we adopted rat puromycin aminonucleoside-induced nephrosis that represents a self-limiting injury of the podocytes and examined the significance of vitamin A and its active metabolites in maintaining the integrity of the podocyte.

Materials and Methods

Reagent and Chemicals

All trans-retinoic acid (ATRA) and puromycin aminonucleoside (PAN) were purchased from Sigma (St. Louis, MO). BMS-189453, a compound that antagonizes all classes of RAR, was supplied by Bristol-Myers-Squibb (Princeton, NJ). Vitamin A-deficient diet modified from AIN-93G (11), which contained less than 0.01 mg retinol/100 g, was purchased from Oriental Yeast (Osaka, Japan). Mouse monoclonal antibody (clone 5-1-6) that recognizes the extracellular domain of rat nephrin and rabbit polyclonal antibody that recognizes the intracellular domain of rat nephrin were prepared as described previously (12). Polyclonal anti-RARα antibody was purchased from Santa Cruz Biotechnology (Santa Cruz, CA).

Animals

Male Sprague-Dawley (SD) rats weighing 200 to 250 g were purchased from Japan SLC (Hamamatsu, Japan). PAN nephrosis was induced by a single intravenous injection of PAN (10 mg/100 g body wt). To rats treated with ATRA, 10 or 20 mg/kg body wt of ATRA was administered subcutaneously once a day from the day of the disease induction through the day of the sacrifice. Equal volume of DMSO was administered subcutaneously to the control rats. Where indicated, vitamin A-deficient diet was started to rats 3 wk before the administration of PAN and was continued throughout the experiments. All procedures were approved by the animal committee of Osaka University School of Medicine.

Tissue Preparation

At the time indicated, rats were anesthetized and sacrificed by intraperitoneal administration of pentobarbital (50 mg/kg body wt). After systemic perfusion with phosphate-buffered saline (PBS), kidneys were removed and were sieved to obtain glomeruli. Alternatively, kidneys were thoroughly perfused with PBS followed by 4% paraformaldehyde (PFA)/PBS and were further fixed by immersion in 4%PFA/PBS for 6 h at 4°C. The tissues were then embedded in OCT compound (Sakura Finetechnical Co., Ltd, Tokyo, Japan) or in paraffin.

Measurement of the Urinary Protein/Creatinine Ratio

Spontaneously voided urine was collected between 2 p.m. and 5 p.m. every 2 d. Concentration of protein and creatinine was measured by using Micro TP Test Wako and Creatinine Test Wako, respectively, according to the instructions (Wako, Osaka, Japan).

Northern Blot Analyses

RNA was extracted with Trizol (Life Technologies, Rockville, MD) according to the manufacturer's instruction, and was subjected to Northern blot analyses (13). Briefly, 10 μg of RNA per lane were separated in 1.2% agarose/formaldehyde gel and were transferred to nylon membrane filters (Hybond N^+; Amersham-Pharmacia Biotech, Little Chalfont, UK). The filter hybridized with 1×10^6 cpm/ml of P^{32}-labeled cDNA probes at 42°C for 12 h were washed twice in 2×SSC/0.1% SDS at room temperature for 15 min, and then twice in 0.2×SSC/0.1% SDS at 65°C for 15 min. After the hybridized probes were stripped off, the filters were rehybridized with a probe for rat glyceroldehyde-3-phosphate-dehydrogenase (GAPDH) as the control.

Reverse Transcription-PCR (RT-PCR)

Semiquantitative RT-PCR was performed as described previously (14). Briefly, 0.4 μg of RNA was converted to single-strand DNA with random primers (Invitrogen, Carlsbad, CA) and SuperScript II (Invitrogen). The DNA was diluted to find a linear range for the following PCR reaction. The DNA was diluted at 1:25 for nephrin, 1:25 for midkine, 1:10 for RARα, 1:1 for RARβ, 1:10 for RXRα, and 1:1 for RXRβ. Each diluted DNA was mixed with 2 μl of 10×PCR buffer (Takara, Tokyo, Japan), 1 μl of dNTP mixture (Takara), 1 μM of forward and reverse primers, and 0.1 μl of Takara *Taq*. Synthetic oligonucleotides described below were used as the primers: for nephrin, 5'-AGCCTCTTGACCATCGCTAA-3' and 5'-CCCAG TCAGCGTGAAGGTAG-3'; for midkine, 5'-CGCGGTGGC-CAAAAAGAAAG-3' and 5'-TG ACTTGGTCTTGGAGGTGC-3'; for RARα, 5'-CAGCCCAGCCACTCAATC CCCAT-3' and 5'-GC-CAGGAGAGAGCAGTCCATCTCAG-3'; for RARβ, 5'-AAAGGG GCAGAGTTTGA TGGAGTTC-3' and 5'-AGCAGGGCTTGTAC ACCGGA-3'; for RXRα, 5'-GTACACAGG AACAGCGCTCA-CAGTG-3' and 5'-TTGAAGAAGAACAGGTGCTCC AGGC-3'; for RXRβ, 5'-ATTCCCGAAGCCCAGACAGCTCCTC-3' and 5'-GCA-CAAAG TCGTTT GCCAGCCCCAG-3'; for GAPDH, 5'-CTCTAC-CCACGGCAAGTTCAA-3' and 5'-GGATGACCTTGCCCACAGC-3'. Twenty-eight cycles of PCR were performed with GeneAmp PCR System 9700 (Applied Biosystems). Annealing temperature was 56°C for nephrin, 54°C for midkine, 55°C for RARα, RARβ, and RXRα, 57°C for RXRβ, and 56°C for GAPDH. The PCR products were separated in 2% agarose gel and visualized with ethidium bromide.

In Situ Hybridization Analysis

Seven-micrometer-thick sections were deparaffinized, rehydrated, and further fixed in 4% PFA/PBS for 20 min at room temperature. The sections were sequentially incubated in 50 mM Tris · HCl (pH 7.4) containing 5 μg/ml of proteinase K and 5 mM of EDTA for 15 min at room temperature, in 0.2 N HCl for 10 min at room temperature, and in 0.25% acetic anhydride/0.1 M Triethanolamine for 10 min at room temperature. The sections were prehybridized with the hybridization buffer (4×SSC/50% formamide/10% dextran sulfate/1×Denhardt solution/2 mM EDTA/denatured salmon sperm DNA [500 ng/ml]) for 1 h at 37°C. Hybridization was performed with 2.5 μg/ml of digoxigenin-labeled cRNA probes in the hybridization buffer at 37°C for 17 h. Once hybridization was completed, the sections were washed in 2×SSC at 50°C for 15 min and were incubated at 37°C for 10 min in 10 mM Tris · HCl (pH 7.5)/1 mM EDTA/0.5 M NaCl/ribonuclease A (20 μg/ml). After being washed twice in 2×SSC at 50°C for 15 min and twice in 0.2×SSC at 50°C for 15 min, digoxigenin was immunologically detected by using DIG Nucleic Acid Detection kit (Boehringer Mannheim) according to the manufacturer's instruction. The sections were counterstained with Vector Methylgreen (Vector, Burlingame, CA).

Immunohistochemistry

For nephrin, 4-μm cryostat sections were incubated with 3% normal horse serum/PBS for 30 min and then with anti-nephrin mono-

clonal antibody 5-1-6 for 2 h. The sections were washed in PBS and then incubated with Texas red-conjugated anti-mouse IgG antibody (Vector) for 1 h. For RARα, 4-μm paraffin sections were incubated with 3% normal gout serum/PBS for 30 min and then with anti-RARα (C-20) antibody (Santa Cruz Biotechnology). After the sections were washed in PBS, they were incubated with biotinylated anti-rabbit IgG antibody. Finally, the sections were washed again and then incubated with VECTASTAIN Elite ABC-horseradish peroxidase Reagents for 30 min. To visualize the signals, the sections were incubated in DAB solution (0.05% of 3,3'-diaminobenzidin tetrahydrochloride, 0.01% of H_2O_2, pH 7.2). These paraffin sections were counterstained with Vector Methylgreen. All images were obtained with Nikon ECLIPSE E600 (Nikon, Tokyo, Japan) connected to a Macintosh computer.

Western Blot Analyses

Isolated glomeruli were lysed in the cell lysis buffer (Cell Signaling Technology, Beverly, MA) using a glass/Teflon homogenizer. The protein concentration of each sample was measured by the BCA Protein Assay Kit (Pierce, Rockford, IL) with the use of bovine serum albumin as the standard. The lysate was mixed with Laemmli sample buffer and was boiled for 10 min and cooled on ice. Twenty micrograms of protein were subjected to SDS-polyacrylamide gel electrophoresis and electroblotted onto a polyvinylidene difluoride membrane (Amersham Pharmacia). The membrane was incubated in 5% skim milk/20 mM Tris · HCl (pH 7.6)-buffered saline (TBS)/0.1% Tween 20, and then in anti-nephrin rabbit polyclonal antibody (1:500) or anti-RARα mouse monoclonal antibody (Santa Cruz) (1:1000). To visualize the signals, the horseradish peroxidase-conjugated anti-rabbit or mouse IgG antibody (Dako) was used at 1: 10000 in combination with the SuperSignal West Pico Chemiluminescent Substrate (Pierce).

Transmission Electron Microscopy

Kidneys were dissected after systemic perfusion of PBS. Immediately, the tissues were fixed in 4% glutaraldehyde for 4 h, postfixed in 1% osmium tetroxide, dehydrated in graded acetones, and embedded in Epon-Araldite. Ultra-thin sections, cut into 0.08-μm thickness and stained with uranyl acetate and lead citrate, were examined with Hitachi H-7100 (Hitachi, Tokyo, Japan).

Construction of Luciferase Reporter Vectors

Human genomic DNA was extracted with DNAzol BD (Life Technologies) from peripheral blood obtained from an informed healthy volunteer. Two kb of the 5'-genomic sequence flanking the transcription start site of human nephrin gene was obtained by PCR with the following primers: 5'-TGAGGCTCGAGAATCGCTTGGACCT-3' and 5'-TTCAGATCTTCCCTGTGAGTATCTC-3'. The PCR product was sequenced and inserted into *XhoI/Bgl*II-cut pGL2-promoter vector that has SV40 promoter positioned on the upstream of *Firefly* luciferase gene (Promega, Madison, WI). A 325-bp fragment covering the region from #-1060 through #-735 was subcloned into *XhoI/Bgl*II-cut pGL2-promoter vector by using PCR with the following primers: 5'-GGAGGCTCAAGCAGATGGATC-3' and 5'-AGCTGGGCCC CCAGATCTTCCTT-3'.

Cell Culture and Luciferase Assay

HeLa cells were cultured in DMEM supplemented with 10% fetal calf serum (FCS), 100 unit/ml penicillin, and 100 μg/ml streptomycin. The cells were seeded on 24-well plates at 1×10^4 cells per well 48 h before the transfection. Plasmid DNA was introduced with TransFast transfection reagent (Promega) according to the manufacturer's instruction. Briefly, the cells cultured in 24-well plates were washed with Opti-MEM (Invitrogen). The cells were transfected with the pGL2-promoter vector harboring the 2-kb promoter region of human nephrin (0.75 μg/well) or the 325-bp region (0.75 μg/well). pRL-TK vector (5 ng/well; Promega), which has the Herpes simplex virus thymidine kinase promoter positioned on the upstream of *Renilla* luciferase gene, was transfected simultaneously to correct the transfection efficiency. The culture medium was switched to DMEM supplemented with 0.5% FCS 4 h after the transfection. After the following 20 h, the cells were stimulated with 10^{-8}, 10^{-7}, 10^{-6}, or 10^{-5} M of ATRA in DMEM supplemented with 0.2% FCS. To inhibit the activity of the RAR family, the cells were stimulated with 10^{-5} M of ATRA in the presence of 10, 1, or 0.1 μM of BMS-189453. Twenty-four hours after the addition of ATRA, the cells were lysed in the Passive Lysis Buffer (Promega) according to the manufacturer's instruction and were subjected to freeze-thaw twice. *Firefly* luciferase activity and *Renilla* luciferase activity were measured with Dual-Luciferase reporter assay system (Promega) and Lumat LB9507 (Berthhold Technologies, Wildbad, Germany) according to the manufacturer's instruction. The results were shown as the ratio of the *Firefly* luciferase activity to the *Renilla* luciferase activity.

Statistical Analyses

Statistical significance between experimental values was evaluated by a non-paired *t* test. Significance was defined as $P < 0.05$.

Results

Induction of RALDH2 in the Podocytes of PAN Nephrosis Rats

To examine whether vitamin A and/or its active metabolites are involved in the regeneration of the foot processes, PAN nephrosis rats were made and the expression level of RALDH2 in the glomeruli was measured by Northern blot analyses. As shown in Figure 1A, RALDH2 was dramatically upregulated in response to the administration of PAN. On day 5, the expression level was ten times higher than that on day 0 and returned to the basal level on day 20 (Figure 1B). *In situ* hybridization, which was applied to the tissue on day 5 of PAN nephrosis rats, revealed that RALDH2 was expressed exclusively in the podocytes (Figure 1C).

Expression of Retinoid Receptors in Glomeruli

ATRA regulates transcription of its target genes through nuclear receptors for retinoids such as RARα, RARβ, RXRα, and RXRβ. Semiquantitative RT-PCR revealed that transcripts of all the receptors were expressed in isolated glomeruli of PAN nephrosis rats, and that RARα was the dominant isoform (Figure 2A). RARα mRNA and its protein product were induced slightly on day 5 of PAN nephrosis, while the expression levels of other receptors remained stable over time (Figure 2, A and B). Both *in situ* hybridization and immunohistochemistry demonstrated that RARα was localized mainly to the podocytes (Figure 2C).

Effects of Exogenous ATRA and Vitamin A–Deficient Diet on PAN Nephrosis

According to our results described above, it was expected that exogenous ATRA or lack of vitamin A (an upstream

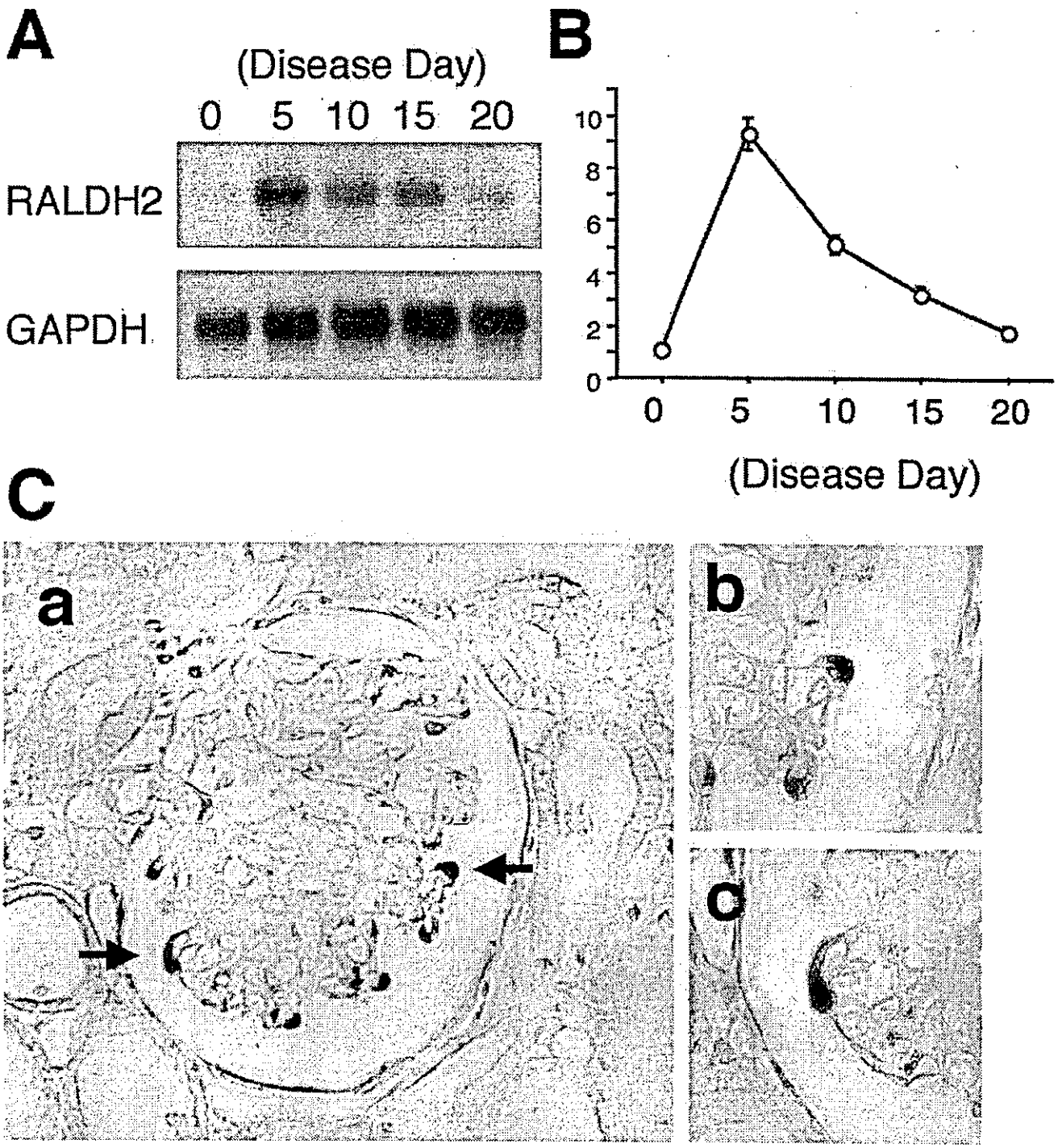

Figure 1. Glomeruli were obtained from puromycin aminonucleoside-induced (PAN) nephrosis rats on days 0, 5, 10, and 20. The expression level of retinaldehyde dehydrogenase type 2 (RALDH2) mRNA was examined by Northern blot analyses. (A) RNA transferred to a filter was probed with the ^{32}P-labeled cDNA probes, and the filter was exposed to a film: a 365-bp *RsaI-StyI* fragment of rat RALDH2 cDNA (upper panel) and a rat GAPDH (lower panel). (B) The autoradiogram was subjected to the densitometry using ImageQuant (Molecular Dynamics). The signal ratio of RALDH2 to GAPDH was shown as the fold increases against the value on day 0 (mean ± SD, $n = 3$). (C) The localization of RALDH2 mRNA was detected by *in situ* hybridization. A 365-bp *RsaI-StyI* fragment of rat RALDH2 was subcloned into pST-Blue1. Antisense and sense digoxigenin (DIG)-labeled cRNA probes were made by using Riboprobe Combination System (Promega). (a) the antisense probe for RALDH2 mRNA (×400). (b and c) the cells pointed by the arrows are shown in higher magnification (×1000). The sense probe for RALDH2 did not show any signals (data not shown).

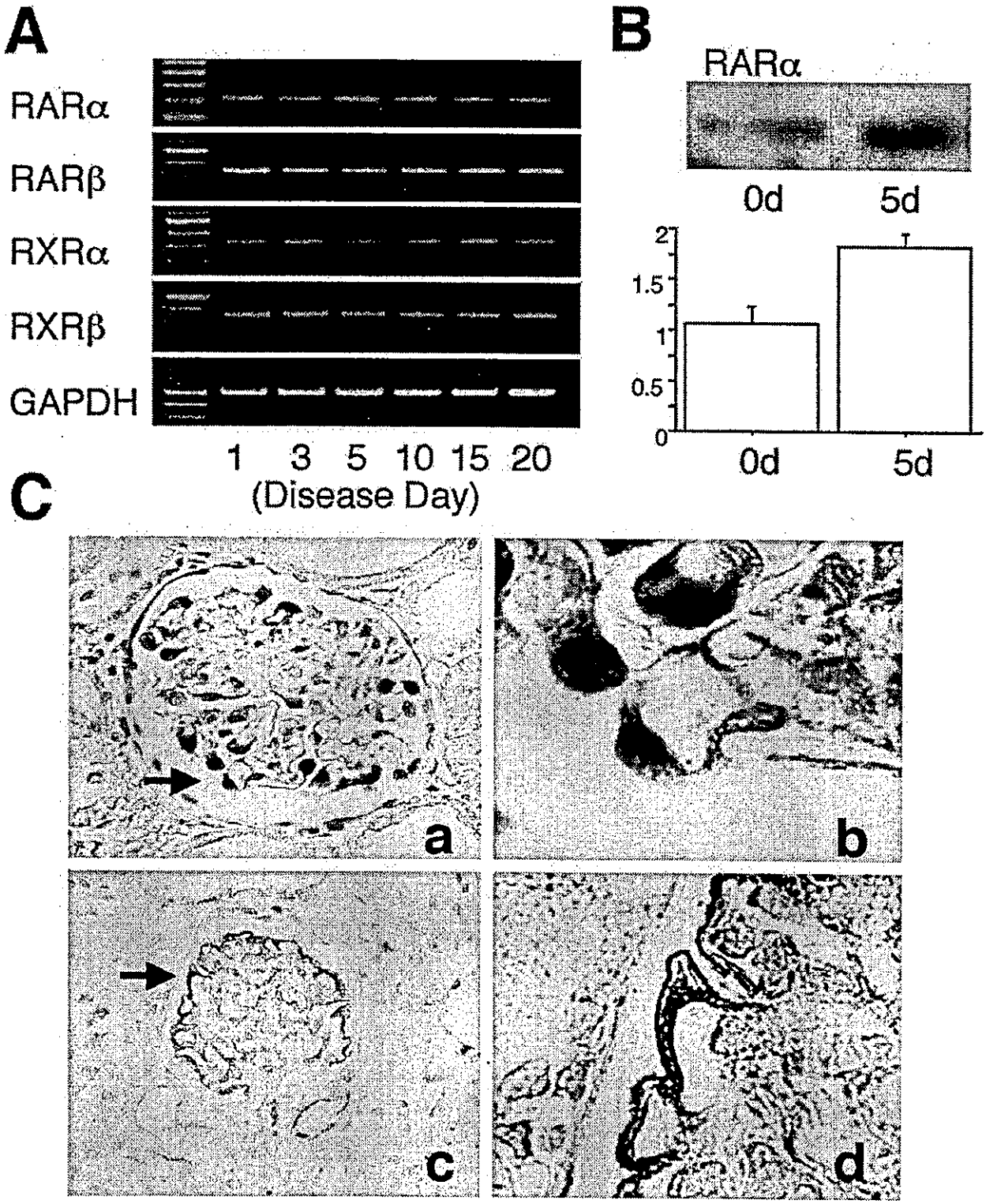

Figure 2. (A) Expression levels of retinoic acid receptor-α (RARα), RARβ, retinoid X receptor-α (RXRα), and RXRβ in isolated glomeruli were examined by RT-PCR. DNA ladder markers are shown in the left lane. (B) Expression level of RARα was examined by Western blot analysis. Twenty micrograms of protein was applied to each lane. (C) Localization of RARα mRNA (a and b) and its protein product (c and d) was examined by *in situ* hybridization and immunohistochemistry, respectively. (a and b) a 202-bp (#1596–#1798) of RARα fragment was subcloned into pSTblue-1. Antisense and sense digoxigenin (DIG)-labeled cRNA probes were made by using Riboprobe Combination System (Promega). The cell pointed by the arrow in (a) (×400) is shown at a higher magnification in (b) (×1000). The sense probe for RARα did not show any signals (data not shown). (c and d) the protein product is also localized to the podocytes (c, ×400; d, ×1000).

substrate of RALDH2) would attenuate the phenotype of PAN nephrosis. From the first day of PAN nephrosis, 10 or 20 mg/kg of ATRA was administered subcutaneously once a day to PAN nephrosis rats. Daily administration of 10 mg/kg of ATRA reduced the urinary protein/creatinine ratio, which was statistically significant on day 15 and thereafter (Figure 3A). When 20 mg/kg of ATRA was used, this beneficial effect was more remarkable and was obtained at an earlier time point (Figure 3A). Consistently, the effacement of the foot processes was less serious in rats treated with ATRA than that in untreated rats (Figure 4). A reciprocal phenotype was obtained in vitamin A–deficient rats. When rats had been fed with a vitamin A–deficient diet from 3 wk before the induction of PAN nephrosis, the urinary protein/creatinine ratio remained high without the spontaneous remission that is normally expected in PAN nephrosis (Figure 3B). Importantly, rats fed with a vitamin A–deficient diet did not develop nephrosis in the absence of the administration of PAN (Figure 3B). These results clearly indicate that the demand for vitamin A and/or its active metabolites such as ATRA increases in response to PAN and that these molecules are indispensable for the repair of the injured podocytes in PAN nephrosis rats.

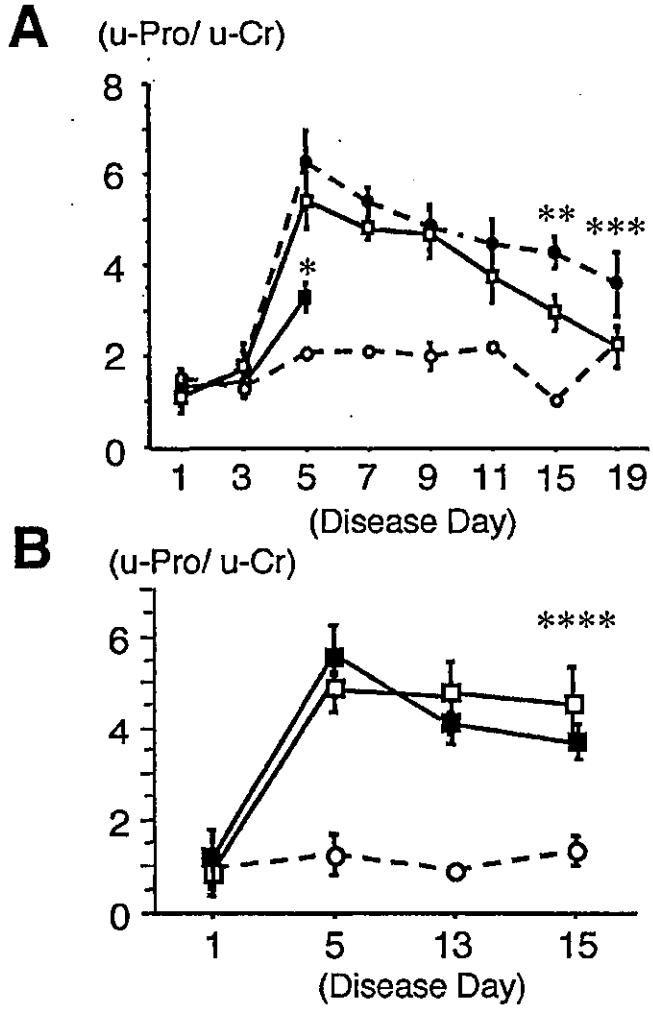

Figure 3. (A) The effect of exogenous ATRA on the urinary protein/creatinine ratio is shown. Broken line with open circles, normal rats; broken line with closed circles, PAN nephrosis rats treated with vehicle alone; solid line with open squares, rats treated with 10 mg/kg of ATRA; solid line with closed squares, rats treated with 20 mg/kg of ATRA. (B) The effect of a vitamin A–deficient diet on the urinary protein/creatinine ratio is shown. Broken line with open circles, normal rats fed with vitamin A–deficient diet; solid line with closed squares, PAN nephrosis rats fed with the normal diet; solid line with open squares, PAN nephrosis rats fed with a vitamin A–deficient diet. The sample number at each time point is three. The values are expressed as mean ± SD. Statistical significance was obtained by comparison with the basal value; * $P < 0.002$; ** $P < 0.002$; *** $P < 0.016$; **** $P < 0.05$.

Expression Levels of Nephrin and Midkine in Glomeruli of PAN Nephrosis Rats

Perturbation of nephrin results in massive proteinuria with the effacement of the foot processes (15,16). The expression level of nephrin decreases in PAN nephrosis rats (17,18). Therefore, we assumed that the administration of ATRA would affect the expression of nephrin in glomeruli of PAN nephrosis rats. Midkine, one of the known target genes of ATRA (19,20) was also examined as a reference for the local concentration of ATRA. Semiquantitative RT-PCR applied on day 0, 3, 5, and 7 of PAN nephrosis revealed that the amount of nephrin mRNA was well maintained in rats treated with ATRA, while it decreased in rats without treatment (Figure 5, top panel). This effect was obvious on day 5 but not on days 3 and 7. Because the response of midkine to ATRA was almost identical to that of nephrin (Figure 5, middle panel), it is likely that ATRA regulates both genes through a common or similar mechanism. The effect of ATRA on nephrin protein product was also confirmed by immunohistochemistry and Western blot analysis. The protein product of nephrin was clearly stained and was localized linearly along the capillary wall of normal glomeruli, which was not affected by the administration of ATRA (Figure 6A, a and b). In the glomeruli of PAN nephrosis rats on day 5, however, only a trace of nephrin was seen (data not shown). Intriguingly, the response of PAN

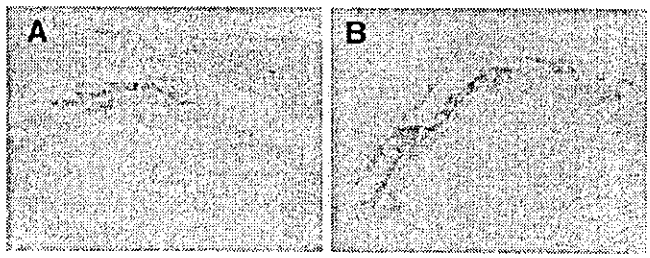

Figure 4. Ultrathin sections of the glomeruli obtained from day 5 of PAN nephrosis were observed by electron microscopy (×15000). (A) rats treated with 20 mg/kg of ATRA; (B) rats treated with vehicle alone. The effacement of the foot processes is less serious in rats treated with ATRA than that in untreated rats. The representative images are shown.

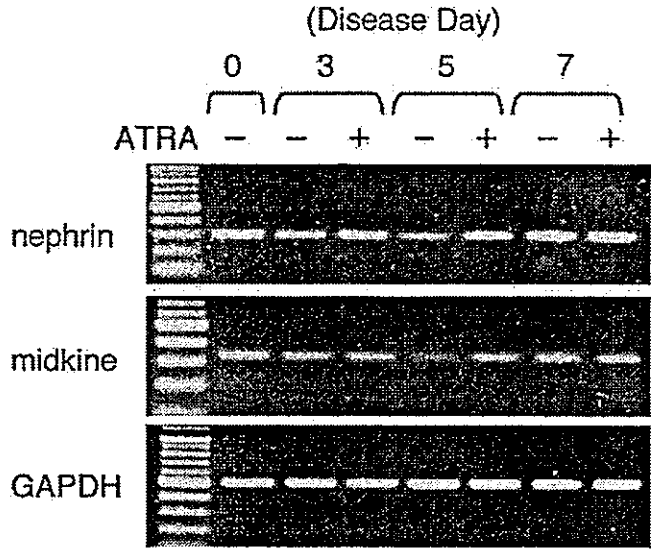

Figure 5. Expression levels of nephrin mRNA (top panel) and midkine mRNA (middle panel) were examined by RT-PCR on days 3, 5, and 7 of the rats treated with 20 mg/kg of ATRA or vehicle alone. PCR products were separated in 2% agarose gel and were stained with ethidium bromide. DNA ladder markers are shown in the left lane. Rat GAPDH was amplified as the control (bottom panel).

nephrosis rats to ATRA presented a striking contrast to that of normal rats. PAN nephrosis rats partially recovered the normal expression pattern of nephrin even though the expression level was still lower than the normal (Figure 6A, c and d). Western blot analyses confirmed that nephrin protein was dramatically reduced in PAN nephrosis rats and that the reduction was mild when rats were treated with ATRA (Figure 6B). These data indicate that ATRA regulates the expression of nephrin mRNA and its protein product.

RARE in the Promoter Region of Human Nephrin Gene

To examine whether ATRA and presumably other active metabolites of vitamin A directly affect the transcription of nephrin gene, we retrieved the sequence of human nephrin gene (NPHS1) from the existing database and analyzed it. As shown in Figure 7, there were at least three putative retinoic acid response elements (RARE) within 2-kb of the promoter region. We made a plasmid construct harboring the 2-kb of the promoter region or the 325-bp fragment including the two putative RARE: (#-774~#-757) and (#-1041~#-1021), and we measured the enhancer activity in HeLa cells. HeLa cells were chosen as the host cell because the cells express several known types of receptors for retinoids (21). Transcriptional activity of the 2-kb promoter region was clearly augmented by ATRA in a dose-dependent manner and increased by fourfold in the presence of 10^{-5} M of ATRA (Figure 8A). Apparently, this activation was achieved through RAR bound to ATRA because BMS-189453, an antagonist for all types of RAR (22), canceled the ATRA-dependent transactivation in a dose-dependent manner (Figure 8B). Putative nonspecific cytotoxicity that might be brought by BMS-189453 did not account for the antagonization because the toxicity, if any, was detected as the decline in the activity of *Renilla* luciferase that was driven independent of ATRA. To further specify the element responding to ATRA, we performed a similar assay using the 325-bp region. As shown in Figure 8A, this region exerted much stronger transcriptional activity than the longer 2-kb region in the presence of ATRA. The maximum activation was achieved at the concentration of 10^{-6} M of ATRA, and the activity did not show any further increase at 10^{-5} M. This result indicates that the 325-bp region contains the RARE as the enhancer.

Discussion

Usefulness of ATRA and other derivatives of vitamin A (retinoids) is confirmed or proposed in a wide range of disease entities such as dermatitis, leukemia, and stenotic arterial diseases (23–27). In proliferating renal diseases, exogenous administration of ATRA, 9-*cis*-retinoic acid, or 13-*cis*-retinoic acid suppresses the proliferation of mesangial cells (26,27). However, even though anti-proteinuric effects are observed in these studies (26,27), the precise modes of action exerted by retinoids and the molecular targets of retinoids remain unknown. In this study, we demonstrated that injured podocytes require ATRA or other related retinoids to repair themselves. In addition, we have revealed a novel molecular mechanism that the podocytes rely on.

The effacement of the foot processes reportedly reached the maximum on day 5 in PAN nephrosis rats, and the amount of proteinuria reached the maximum on day 5 (28). The temporal expression pattern of RALDH2 closely correlated to the perturbation of the normal glomerular functions and structures (Figure 1) (28). Therefore, it is most likely that injured podocytes elevated the intracellular concentration of ATRA using the catalytic activity of RALDH2 that is upregulated in their own cell bodies. We also found out that RALDH2 was expressed in the developing renal epithelium such as the comma-shaped body, the S-shaped body, and weakly in the capillary loop stage epithelium (unpublished data), which suggested RALDH2 might be essential for podocyte development. The localization of RARα supports the significance of ATRA in the podocytes (Figure 2). Now, what is the role of ATRA in the podocytes?

The normal structure of the slit diaphragm is essential for preventing serum protein from leaking out of glomerular capillaries. Disruption of the slit diaphragm is histologically recognized as the effacement of the foot processes projected by the podocytes, which is typically observed in human nephrotic syndrome such as minimal change nephrotic syndrome (MCNS). In response to appropriate therapy including the administration of glucocorticoid, proteinuria in MCNS ameliorates along with the recovery of the slit diaphragm. PAN nephrosis, which is accompanied by the foot process effacement and focal detachment of podocytes from the glomerular basement membrane (GBM) (29,30), mimics human MCNS, at least in a sense that PAN nephrosis shows temporal massive proteinuria and subsequent complete remission without any scar in the kidney. Many investigators have studied the molecular mechanisms of PAN-induced proteinuria (31–35) and

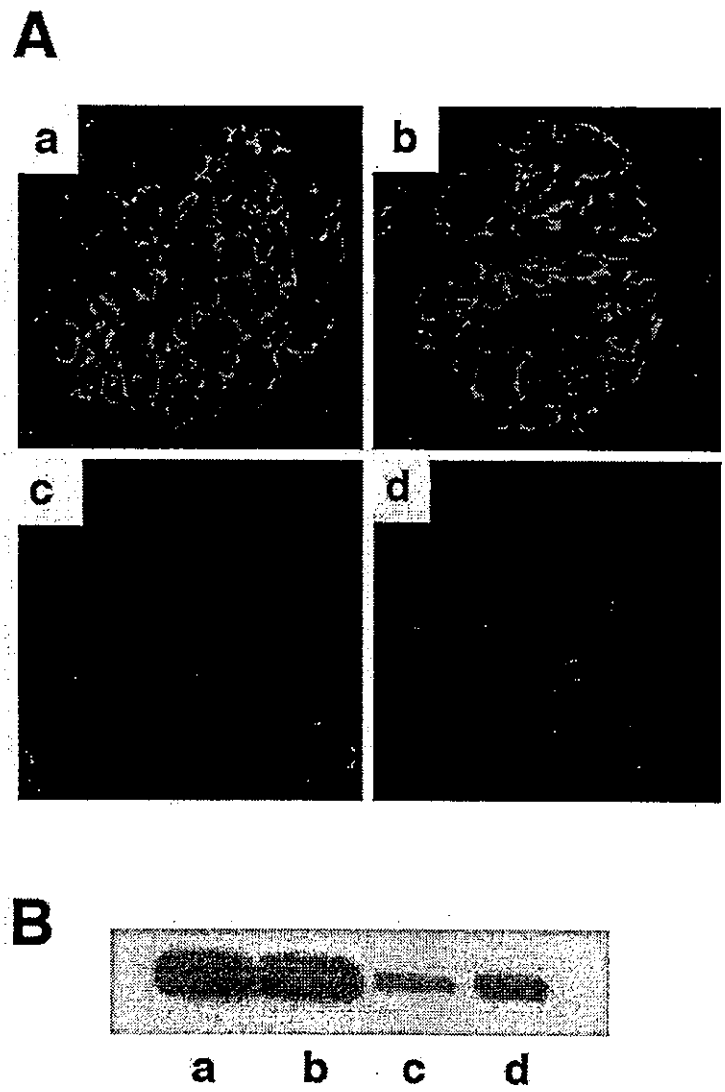

Figure 6. (A) Immunofluorescence image of nephrin. Kidney sections prepared from normal rats, normal rats treated with ATRA, PAN nephrotic rats on day 5, and PAN nephrotic rats treated with ATRA on day 5 were stained with anti-nephrin antibody in combination with Texas Red-conjugated secondary antibody. (a) Normal rats treated with vehicle alone (×400). (b) Normal rats treated with 20 mg/kg of ATRA (×400). (c) PAN nephrotic rats treated with vehicle alone (×400). (d) PAN nephrotic rats treated with 20 mg/kg of ATRA (×400). (B) Western blot analyses of nephrin. Glomeruli were isolated from the four groups of rats. Twenty milligrams of protein was subjected to each lane. Lane a, normal rats treated with vehicle alone; lane b, normal rats treated with 20 mg/kg of ATRA; lane c, PAN nephrotic rats treated with vehicle alone; lane d, PAN nephrotic rats treated with 20 mg/kg of ATRA.

demonstrated that nephrin is one of the most responsible genes (12,17). Nephrin, discovered as the gene whose mutation causes Finnish type of congenital nephrotic syndrome (36), is localized to the slit diaphragm.

We demonstrated here that ATRA directly enhance the transcription of nephrin gene (Figure 8). However, there are several mechanisms how ATRA and other retinoids regulate the target genes. The first mechanism is through a change in the rate of gene transcription (37). The second one involves a change in the stability or half-life of a particular mRNA in response to retinoids (38). In addition, the transcriptional regulation by ATRA can be divided into two types, the direct one and the indirect one. The direct regulation by ATRA is generally rapid and mediated through direct binding of RAR or RAR-RXR complexes to the RARE (37). On the contrary, the indirect regulation appears later, and no direct binding of RAR or RAR-RXR to the RARE is observed (37). Whereas ATRA enhanced the transcription of nephrin through the direct regulation, we have no data to know whether ATRA changes the stability or half-life of nephrin mRNA. The 2-kb promoter region of human nephrin gene has three feasible RARE, one direct repeat, one palindrome, and one complex type (Figure 7). Each element matches the consensus sequence with minor variation, which suggests that each of the regions has a weak

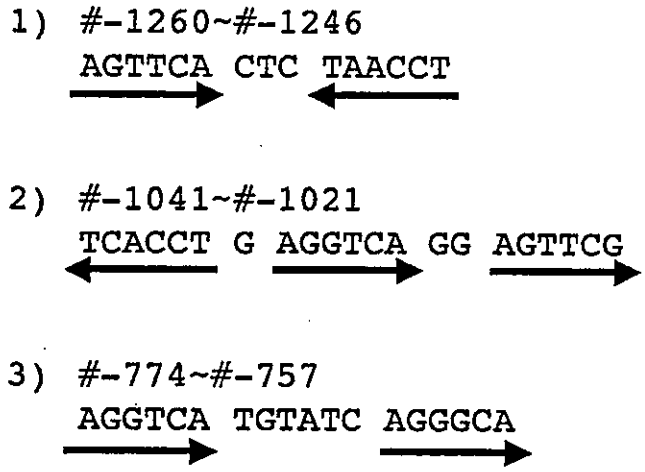

Figure 7. The 2-kb promoter region of the human nephrin gene (NPHS1) was retrieved from the existing database and analyzed. Three putative retinoic acid response elements (RARE) are found. The numbers indicate the position of the nucleotide counted from the transcriptional start site that is reported by Wong *et al.* (48).

response to ATRA. According to our results obtained from HeLa cells, at least the region #-1041 through #-1021, the region #-774 through #-757, or both are the functional RARE (Figure 8). If cells expressing transacting factors essential for nephrin were used instead of HeLa cells, the response to ATRA would be more remarkable.

Although the demand for ATRA increases during the repair process of the injured podocytes, those might result from temporally increased consumption of retinoids within the cells. Given the case, one possible explanation is that oxidative stress in glomeruli of PAN nephrosis rats (39) could lead to acute degradation of retinoids and to lack of retinoids because the oxidation step through CYP26 is one of the natural degradation mechanisms for ATRA (40). This is an intriguing hypothesis that might account for the perturbation of the slit diaphragm in PAN nephrosis or other podocyte injuries. However, our result that normal rats fed with a vitamin A–deficient diet did not spontaneously develop nephrosis implies that the low concentration of ATRA in the podocytes is not a direct cause of the perturbed slit diaphragm. Because it is difficult to measure the intracellular concentration of ATRA and/or other retinoids in the podocytes, different strategies will be required to address this question. It is reported that the distribution of RALDH2 provides the most accurate guide to the localization of ATRA (41–44). Therefore, studying the transcriptional regulation of RALDH2 gene might be informative to further understand the temporal change of intracellular concentration of ATRA.

We propose a mechanism that the injured podocytes take on to repair the disturbed slit diaphragm. First, the core system to produce active metabolites of vitamin A is upregulated. At this point, sufficient amount of the substrates such as vitamin A and β-carotene are required as the substrate. It can be expected that the significant lack of vitamin A retard the repair. Second, active metabolites including ATRA bind to retinoid receptors

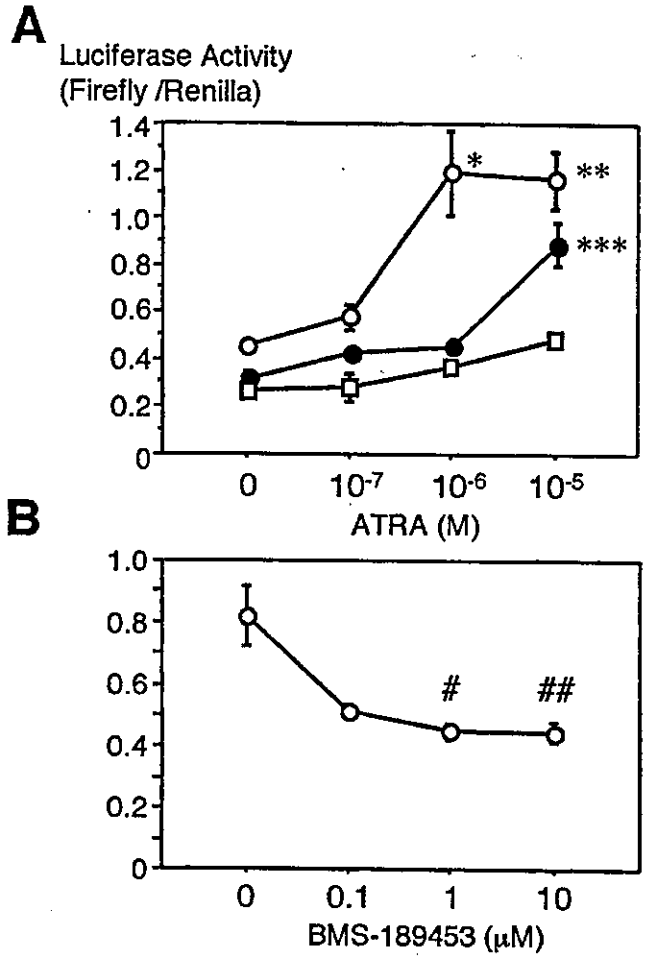

Figure 8. The enhancer activity of the 2-kb and the 325-bp promoter regions (#-1060 through #-735) was examined as described in Materials and Methods. (A) HeLa cells transfected with the *Firefly* luciferase reporter plasmid harboring the 2-kb region (closed circles) or the 325-bp region (open circles) was stimulated with various concentration of ATRA. The pGL-2 promoter vector was transfected to the cells as a control (open squares). (B) Luciferase assay was performed in the presence of various concentration of BMS-189453 by using the plasmid harboring the 2-kb promoter region. Transfection efficiency was adjusted by the activity of the cotransfected *Renilla* luciferase. The results are shown as the ratio of *Firefly* luciferase activity to *Renilla* luciferase activity (mean ± SD; $n = 3$ at each points). Each values was compared with the basal value, and the statistical significance was indicated as follows: * $P < 0.04$; ** $P < 0.04$; *** $P < 0.02$; # $P < 0.05$; ## $P < 0.05$.

that are constitutively expressed in the podocytes and then transcribe their target genes. Similar mechanisms might work in human diseases because the expression of nephrin also decreases in human acquired nephrotic syndrome (45–47). In addition, ATRA might play a direct role to organize the structural components for the slit diaphragm. Our results also suggest that the disturbance of the retinoids signaling in the podocytes could be one of causes leading to progressing renal diseases.

Acknowledgments

We thank Naoko Horimoto for technical assistance and Bristol-Myers-Squibb for providing BMS-189453. This research was supported by a Grant-in Aid for Scientific Research from the Ministry of Education, Science and Culture, Japan, and by a grant from Takeda Medical Research Foundation.

References

1. Chambon P: A decade of molecular biology of retinoic acid receptors. *Faseb J* 10: 940–954, 1996
2. Niederreither K, Subbarayan V, Dolle P, Chambon P: Embryonic retinoic acid synthesis is essential for early mouse post-implantation development. *Nat Genet* 21: 444–448, 2001
3. Boncinelli E, Simeone A, Acampora D, Mavilio F: HOX gene activation by retinoic acid. *Trends Genet* 7: 329–334, 1991
4. Boncinelli E, Simeone A, Acampora D, Gulisano M: Homeobox genes in the developing central nervous system. *Ann Genet* 36: 30–37, 1993
5. Sporn MB, Roberts AB, Goodman DS: *The Retinoids*, 2nd ed, New York, Raven Press, Ltd., 1994
6. Wilson J, Roth C, Warkany J: An analysis of the syndrome of malformations induced by maternal vitamin A deficiency. *Am J Anat* 92: 189–217, 1953
7. Lelievre-Pegorier M, Vilar J, Ferrier M, Moreau E, Freund N, Gilbert T, Merlet-Benichou C: Mild vitamin A deficiency leads to inborn nephron deficit in the rat. *Kidney Int* 54: 1455–1462, 1998
8. Batourina E, Gim S, Bello N, Shy M, Clagett-Dame M, Srinivas S, Costantini F, Mendelsohn C: Vitamin A controls epithelial/mesenchymal interactions through Ret expression. *Nat Genet* 27: 74–78, 2001
9. Mendelsohn C, Batourina E, Fung S, Gilbert T, Dodd J: Stromal cells mediate retinoid-dependent functions essential for renal development. *Development* 126: 1139–1148, 1999
10. Moreau E, Vilar J, Lelievre-Pegorier M, Merlet-Benichou C, Gilbert T: Regulation of c-ret expression by retinoic acid in rat metanephros: Implication in nephron mass control. *Am J Physiol* 275: F938–F945, 1998
11. Gardner EM, Ross AC: Dietary vitamin A restriction produces marginal vitamin A status in young rats. *J Nutr* 123: 1435–1443, 1993
12. Kawachi H, Koike H, Kurihara H, Yaoita E, Orikasa M, Shia MA, Sakai T, Yamamoto T, Salant DJ, Shimizu F: Cloning of rat nephrin: Expression in developing glomeruli and in proteinuric states. *Kidney Int* 57: 1949–1961, 2000
13. Maniatis T, Frisch E, Sambrook J: Molecular cloning, in *Molecular Cloning*, Vol 1, 2nd ed, edited by Ford N, New York, Cold Spring Harbor Laboratory Press, 1989: pp 7.3–7.79
14. Nagatoya K, Moriyama T, Kawada N, Takeji M, Oseto S, Murozono T, Ando A, Imai E, Hori M: Y-27632 prevents tubulointerstitial fibrosis in mouse kidneys with unilateral ureteral obstruction. *Kidney Int* 61: 1684–1695, 2002
15. Orikasa M, Matsui K, Oite T, Shimizu F: Massive proteinuria induced in rats by a single intravenous injection of a monoclonal antibody. *J Immunol* 141: 807–814, 1988
16. Topham PS, Kawachi H, Haydar SA, Chugh S, Addona TA, Charron KB, Holzman LB, Shia M, Shimizu F, Salant DJ: Nephritogenic mAb 5–1-6 is directed at the extracellular domain of rat nephrin. *J Clin Invest* 104: 1559–1566, 1999
17. Luimula P, Ahola H, Wang SX, Solin ML, Aaltonen P, Tikkanen I, Kerjaschki D, Holthofer H: Nephrin in experimental glomerular disease. *Kidney Int* 58: 1461–1468, 2000
18. Luimula P, Aaltonen P, Ahola H, Palmen T, Holthofer H: Alternatively spliced nephrin in experimental glomerular disease of the rat. *Pediatr Res* 48: 759–762, 2000
19. Muramatsu T: Midkine (MK), the product of a retinoic acid responsive gene, and pleiotrophin constitute a new protein family regulating growth and differentiation. *Int J Dev Biol* 37: 183–188, 1993
20. Mitsiadis T, Muramatsu T, Muramatsu H, Thesleff I: Midkine (MK), a heparin-binding growth/differentiation factor, is regulated by retinoic acid and epithelial-mesenchymal interactions in the developing mouse tooth, and affects cell proliferation and morphogenesis. *J Cell Biol* 129: 267–281, 1995
21. Leid M, Kastner P, Lyons R, Nakshatri H, Saunders M, Zacharewski T, Chen JY, Staub A, Garnier JM, Mader S: Purification, cloning, and RXR identity of the HeLa cell factor with which RAR or TR heterodimerizes to bind target sequences efficiently: *Cell* 68: 377–395, 1992
22. Schulze GE, Clay RJ, Mezza LE, Bregman CL, Buroker RA, Frantz JD: BMS-189453, a novel retinoid receptor antagonist, is a potent testicular toxin: *Toxicol Sci* 59: 297–308, 2001
23. Wiegman PJ, Barry WL, McPherson JA, McNamara CA, Gimple LW, Sanders JM, Bishop GG, Powers ER, Ragosta M, Owens GK, Sarembock IJ: All-trans-retinoic acid limits restenosis after balloon angioplasty in the focally atherosclerotic rabbit : a favorable effect on vessel remodeling. *Arterioscler Thromb Vasc Biol* 20: 89–95, 2000
24. Fontana JA, Rishi AK: Classical and novel retinoids: Their targets in cancer therapy. *Leukemia* 16: 463–472, 2002
25. Gollnick H, Schramm M: Topical drug treatment in acne. *Dermatology* 196: 119–125, 1998
26. Wagner J, Dechow C, Morath C, Lehrke I, Amann K, Waldherr R, Floege J, Ritz E: Retinoic acid reduces glomerular injury in a rat model of glomerular damage. *J Am Soc Nephrol* 11: 1479–1487, 2000
27. Schaier M, Lehrke I, Schade K, Morath C, Shimizu F, Kawachi H, Grone HJ, Ritz E, Wagner J: Isotretinoin alleviates renal damage in rat chronic glomerulonephritis. *Kidney Int* 60: 2222–2234, 2001
28. Inokuchi S, Shirato I, Kobayashi N, Koide H, Tomino Y, Sakai T: Re-evaluation of foot process effacement in acute puromycin aminonucleoside nephrosis. *Kidney Int* 50: 1278–1287, 1996
29. Ryan GB, Karnovsky MJ: An ultrastructural study of the mechanisms of proteinuria in aminonucleoside nephrosis. *Kidney Int* 8: 219–232, 1975
30. Caulfield JP, Reid JJ, Farquhar MG: Alterations of the glomerular epithelium in acute aminonucleoside nephrosis. Evidence for formation of occluding junctions and epithelial cell detachment. *Lab Invest* 34: 43–59, 1976
31. Breiteneder-Geleff S, Matsui K, Soleiman A, Meraner P, Poczewski H, Kalt R, Schaffner G, Kerjaschki D: Podoplanin, novel 43-kd membrane protein of glomerular epithelial cells, is downregulated in puromycin nephrosis. *Am J Pathol* 151: 1141–1152, 1997
32. Krishnamurti U, Zhou B, Fan WW, Tsilibary E, Wayner E, Kim Y, Kashtan CE, Michael A: Puromycin aminonucleoside suppresses integrin expression in cultured glomerular epithelial cells. *J Am Soc Nephrol* 12: 758–766, 2001
33. Walker LM, Shah SV, Mayeux PR: Lack of a role for inducible nitric oxide synthase in an experimental model of nephrotic syndrome. *Biochem Pharmacol* 60: 137–143, 2000

34. Levidiotis V, Kanellis J, Ierino FL, Power DA: Increased expression of heparanase in puromycin aminonucleoside nephrosis. *Kidney Int* 60: 1287–1296, 2001
35. Smoyer WE, Mundel P, Gupta A, Welsh MJ: Podocyte alpha-actinin induction precedes foot process effacement in experimental nephrotic syndrome. *Am J Physiol* 273: F150–F157, 1997
36. Kestila M, Lenkkeri U, Mannikko M, Lamerdin J, McCready P, Putaala H, Ruotsalainen V, Morita T, Nissinen M, Herva R, Kashtan CE, Peltonen L, Holmberg C, Olsen A, Tryggvason K: Positionally cloned gene for a novel glomerular protein–nephrin–is mutated in congenital nephrotic syndrome. *Mol Cell* 1: 575–582, 1998
37. Sporn MB, Roberts AB, Goodman DS: The retinoids, In: *Biology, Chemistry and Medicine*, 2nd ed, edited by Goodman DS, New York, Raven Press, 1994
38. Busam KJ, Geiser AG, Roberts AB, Sporn MB: Synergistic increase of phorbol ester-induced c-fos mRNA expression by retinoic acid through stabilization of the c-fos message. *Oncogene* 8: 2267–2273, 1993
39. Ricardo SD, Bertram JF, Ryan GB: Reactive oxygen species in puromycin aminonucleoside nephrosis: In vitro studies. *Kidney Int* 45: 1057–1069, 1994
40. White JA, Beckett-Jones B, Guo YD, Dilworth FJ, Bonasoro J, Jones G, Petkovich M: cDNA cloning of human retinoic acid-metabolizing enzyme (hP450RAI) identifies a novel family of cytochromes P450. *J Biol Chem* 272: 18538–18541, 1997
41. Ulven S, Gundersen T, Weedon M, Landaas V, Sakhi A, Fromm S, Geronimo B, Moskaug J, Blomhoff R: Identification of endogenous retinoids, enzymes, binding proteins, and receptors during early postimplantation development in mouse: Important role of retinal dehydrogenase type 2 in synthesis of all-trans-retinoic acid. *Dev Biol* 220: 379–391, 2000
42. Ross S, McCaffery P, Drager U, De Luca L: Retinoids in embryonal development. *Physiol Rev* 80: 1021–1054, 2000
43. Berggren K, McCaffery P, Drager U, Forehand C: Differential distribution of retinoic acid synthesis in the chicken embryo as determined by immunolocalization of the retinoic acid synthetic enzyme, RALDH-2. *Dev Biol* 210: 288–304, 1999
44. Niederreither K, McCaffery P, Drager U, Chambon P, Dolle P: Restricted expression and retinoic acid-induced downregulation of the retinaldehyde dehydrogenase type 2 (RALDH-2) gene during mouse development. *Mech Dev* 62: 67–78, 1997
45. Furness PN, Hall LL, Shaw JA, Pringle JH: Glomerular expression of nephrin is decreased in acquired human nephrotic syndrome. *Nephrol Dial Transplant* 14: 1234–1237, 1999
46. Huh W, Kim DJ, Kim MK, Kim YG, Oh HY, Ruotsalainen V, Tryggvason K: Expression of nephrin in acquired human glomerular disease. *Nephrol Dial Transplant* 17: 478–484, 2002
47. Wang SX, Rastaldi MP, Patari A, Ahola H, Heikkila E, Holthofer H: Patterns of nephrin and a new proteinuria-associated protein expression in human renal diseases. *Kidney Int* 61: 141–147, 2002
48. Wong MA, Cui S, Quaggin SE: Identification and characterization of a glomerular-specific promoter from the human nephrin gene. *Am J Physiol Renal Physiol* 279: F1027–1032, 2000

J Am Soc Nephrol 14: 1223–1233, 2003

Expression and Function of the Developmental Gene Wnt-4 during Experimental Acute Renal Failure in Rats

YOSHIO TERADA, HIROYUKI TANAKA, TOMOKAZU OKADO, HARUKO SHIMAMURA, SEIJI INOSHITA, MICHIO KUWAHARA, and SEI SASAKI
Homeostasis Medicine and Nephrology, Tokyo Medical and Dental University, Tokyo, Japan.

Abstract. The Wnt-β-catenin pathway plays key roles in embryogenesis. Wnt-4 is known to be expressed in the mesonephric duct in embryonic development. It is tempting to speculate that the Wnt-4-β-catenin pathway contributes to the recovery from acute renal failure (ARF). This study used an *in vivo* model of ARF rats to clarify the significance of the Wnt-4-β-catenin pathway in ARF. ARF was induced by clamping the rat left renal artery for 1 h. At 3, 6, 12, 24, 48, and 72 h after reperfusion, whole kidney homogenate and total RNA were extracted for examination by Western blot analysis and real-time RT-PCR. Wnt-4 mRNA and protein expression were strongly increased at 3 to 12 h and 6 to 24 h after ischemia, respectively. In immunohistologic examination, Wnt-4 was expressed in the proximal tubules and co-expressed with aquaporin-1, GM130, and PCNA. Cyclin D1 and cyclin A were expressed at 24 to 48 h after reperfusion. In addition, the overexpression of Wnt-4 and β-catenin promoted the cell cycle and increased the promoter activity and protein expression of cyclin D1 in LLC-PK1 cells. Taken together, these data suggest that the Wnt-4-β-catenin pathway plays a key role in the cell cycle progression of renal tubules in ARF. The Wnt-4-β-catenin pathway may regulate the transcription of cyclin D1 and control the regeneration of renal tubules in ARF.

Ischemic acute renal failure (ARF) is the most common form of ARF in the adult population. The molecular mechanisms of tubular regeneration after ischemic renal injury remain largely unknown (1–3). An understanding of the mechanisms that lead to renal cell proliferation and regeneration will be necessary for the exploration of novel therapeutic strategies for the treatment of ischemic ARF. Some reports have proposed that regeneration processes may recapitulate developmental processes to restore organ or tissue function (4,5). The adult tubular epithelial cells have a potent ability to regenerate after cellular damage. Under a condition of ischemic renal damage, normally quiescent cells undergo de-differentiation and acquire the ability to proliferate after their DNA synthesis is enhanced (6,7). The regulation of cyclin and cyclin-dependent kinase (CDK) inhibitor has been reported in ARF (8,9). The restriction point of the G1-to-S phase is determined by the activities of cyclin D1, cyclin A, cyclin E, and CDK (10,11). Cyclin D1 and cyclin A play key roles in G1-S regulation of renal tubular epithelial cells (12).

Members of the Wnt family of signaling molecules have been shown to have dramatic effects on the induction of metanephric mesenchyme. Wnt are cell-surface molecules that bind to and receptors of the "frizzled" class and activate them (13,14). In early organ culture experiments, Wnt-frizzled interactions appeared to form the base requirement for cell-cell contact between metanephric mesenchyme and inducer tissue (15). Among the Wnt family, Wnt-4 is expressed in developing kidney and may initiate differentiation of the metanephric mesenchyme (15). Mutant mice lacking Wnt-4 show a complete lack of tubular development despite initially normal ureteric bud branching and aggregation of cells at ureteric bud tips, indicating that Wnt-4 is necessary for induction (15). The mutant Wnt4 −/− metanephric mesenchyme can be induced with exogenous Wnt-4 into a substantial portion of the epithelialization pathway, suggesting that Wnt-4 is sufficient for induction (15). In the proposed pathway for Wnt signaling, the inhibition of glycogen synthase kinase (GSK)-3β leads to posttranscriptional stabilization of soluble β-catenin, which in turn leads to the accumulation of β-catenin in the cytoplasm and nucleus (13,14,16). Within the nucleus, β-catenin interacts with members of the TCF (T cell factor)/LEF family of transcription factors to regulate gene expression (17,18). Tetsu and McCormick (19) recently reported that β-catenin activates transcription from the cyclin D1 promoter and that sequences within the promoter related to consensus TCF/LEF-binding sites are required for activation in colon carcinoma cells.

In this study, we hypothesized that the developmental gene, Wnt-4, is re-expressed during regeneration after acute renal failure and plays a key role in transcriptional regulation of cyclin D1 and cell cycle progression in renal tubular cells. To test this hypothesis, we examined the expression pattern of Wnt-4 expression during the recovery phase of ischemia/reperfusion kidney. Our data demonstrate that Wnt-4 is upregulated in the early phase of ischemia/reperfusion kidney, and that the

Received February 26, 2002. Accepted January 23, 2003.
Correspondence to Dr. Yoshio Terada, Homeostasis Medicine and Nephrology, Tokyo Medical and Dental University, 5-45, Yushima 1-chome, Bunkyo-ku, Tokyo 113-8519, Japan. Phone: 81-3-5803-5214; Fax: 81-3-5803-5215; E-Mail: yterada.kid@tmd.ac.jp
1046-6673/1405-1223
Journal of the American Society of Nephrology

DOI: 10.1097/01.ASN.0000060577.94532.06

Wnt-4-β-catenin pathway regulates the transcription of cyclin D1 and cell cycle progression in renal tubules in ARF.

Materials and Methods

Induction of ARF

Male Sprague-Dawley (SD) rats (Saitama Experimental Animal Supply, Saitama, Japan) weighing 150 to 200 g were anesthetized intraperitoneally with sodium pentobarbital (30 mg/kg), and the left renal arteries were occluded with Sugita aneurysm clips (Mizuho Ikakogyo, Tokyo, Japan) for 60 min. The clamps were removed, the incisions were closed, and the rats were sacrificed at 0, 3, 6, 12, 24, 48, 72, and 96 h ($n = 5$). The left kidneys were quickly removed and processed for histologic evaluation, protein extraction, or RNA extraction. Age-matched and weight-matched SD rats that received sham operations without clamping of the renal arteries served as normal controls ($n = 5$). All animal experiments described here were conducted in accordance with the NIH Guide for the Care and Use of Laboratory Animals and approved by the Tokyo Medical and Dental University Review Boards (#0010277).

Isolation of Kidney Tissue and Histologic Examination

Rats were anesthetized with pentobarbital at indicated times after the ischemic event. After perfusing their kidneys with sterile phosphate-buffered saline (PBS), the left kidneys were quickly excised, frozen in liquid nitrogen, and homogenized in the SDS sample buffer described later. For immunohistochemical studies, kidneys were removed after *in vitro* perfusion with 4% paraformaldehyde in a phosphate buffer and immersed overnight in the same fixative at 4°C. The fixed tissue was cryoprotected by immersion in 20% sucrose in PBS at 4°C and then shock-frozen in liquid nitrogen. Frozen 10-μm sections were cut with cryostat, thaw-settled on APS-coated slides, mounted with an aqueous mounting medium (Mount-Quick Aqueous; Daido Sangyo, Tokyo, Japan), and examined under a confocal laser microscope (Carl Zeiss Japan, Tokyo, Japan).

Frozen sections prepared in the manner described above were used for immunohistochemistry. The primary antibodies included anti-Wnt-4 antibody, anti-PCNA–specific antibody (Santa Cruz Biochemical Inc. Santa Cruz, CA), anti-GM130–specific antibody (Transduction Laboratories, San Jose, CA) as a marker for golgi (20), and an aquaporin-1–specific antibody (Santa Cruz Biochemical Inc.) as a marker for proximal tubules (21–23). The blocking peptide for the Wnt-4 antibody was purchased from Santa Cruz Biochemical Inc. The anti-Wnt-4 antibody was generated in goat. The anti-PCNA antibody and the anti-GM130 antibody were mouse monoclonal antibodies. The anti-aquaporin-1 antibody was generated in rabbits. The secondary antibody for the anti-Wnt 4 antibody was an anti-goat IgG FITC-conjugated antibody (Sigma, St. Louis, MO). The secondary antibody for the anti-PCNA antibody and the anti-GM130 antibody was an anti-mouse IgG Cy3-conjugated antibody (Sigma). The anti-aquaporin-1 antibody was an anti-rabbit IgG Cy3-conjugated antibody (Sigma).

After blocking, frozen sections were incubated at room temperature for 1 h with the anti-Wnt 4, anti-PCNA, anti-GM130, and anti-aquaporin-1 antibodies at dilutions of 1:100. The sections were then washed several times and incubated at room temperature for 1 h with the secondary antibodies at dilutions of 1:200. After more washing, the slides were mounted and examined under a confocal laser microscope.

Western Blot Analysis

Homogenized total renal tissue or LLC-PK1 cells were lysed in SDS sample buffer (50 mM Hepes, pH 7.5, 150 mM NaCl, 1.5 mM $MgCl_2$, 1 mM EGTA, 10% glycerol, 1% Triton X-100, 1 μg/ml aprotinin, 1 μg/ml leupeptin, 1 mM phenylmethylsulfonyl fluoride, 0.1 mM sodium orthovanadate) at 4°C (24). Protein was transferred to nitrocellulose membrane and probed with polyclonal antibodies against Wnt-4, cyclin D1, cyclin A, and actin (Santa Cruz Biotechnology). The primary antibodies were detected using horseradish peroxidase (HRP)–conjugated rabbit anti-mouse IgG and visualized by the Amersham ECL system (Amersham Corp., Arlington Heights, IL).

Real-Time Quantitative PCR

Reverse transcription-PCR (RT-PCR) reaction was used to investigate Wnt-4 from RNA extracted from the renal cortices of ischemia/reperfusion kidneys. The RNA was extracted from the renal cortex using TRI-REAGENT (Life Technologies, Gaithersburg, MD) (25). One microgram of total RNA was used for RT-PCR as follows. The real-time quantitative PCR method was used to accurately detect the changes of Wnt-4 gene copies. The cycle at which the amplification plot crosses the threshold (CT) is known to accurately reflect relative mRNA values (26,27). Total RNA was harvested from renal tissue. Rat Wnt-4 and GAPDH mRNAs were amplified. Wnt-4 primer 1 (antisense) encompassed bases 343 to 362, and primer 2 (sense) encompassed bases −4 to 16 (Genebank accession No. AF188698). The sequence of primer 1 was 5'-ATGGAGCCGATCCGGTCCAG-3', and the sequence of primer 2 was 5'-CACCATGCACCTCTC-CCAGC-3'. The predominant cDNA amplification product was predicted to be 366 bp in length (the distance between primers plus the primer length). RT and PCR of glyceraldehyde-3-phosphate-dehydrogenase (GAPDH) served as positive controls. The primers were defined by the following cDNA base sequences (28): primer 1 (antisense), bases 795 to 814, sequence, 5'-AGATCCACAACGG-ATACATT-3'; primer 2 (sense), bases 506 to 525, sequence, 5'-TCCCTCAAGATTGTCAGCAA-3'. The predominant cDNA amplification product was predicted to be 309 bp in length. PCR products were detected and quantitated in real time using the LightCycler Real time PCR (Roche Molecular Biochemicals, Tokyo, Japan) as described previously (26,27). The amplification mixture contained 5 nM of template DNA and 50 μM of primer DNA in 50 nM salt and 1 mM Mg (2) A three-step PCR consisting of denaturation at 94°C for 20 s, annealing at 55°C for 20 s, and extension at 72°C for 30 s was performed for 35 cycles. The reaction produced a 366-bp PCR product for Wnt-4 and a 309-bp product for GAPDH. The PCR cycle at which the amplification plot crossed a threshold of 10 SD above the baseline was defined as the CT value. While the normalized reporter signal remained unchanged in control sample without RNA, the PCR amplification climbed to the threshold value in the sample treated with RNA from renal tissue. In calculating the relative mRNA level, the CT values were assumed to increase by approximately 1 for each twofold dilution. To examine the precision of the assay, mRNA from renal tissue was reverse-transcribed and amplified on three separate days. The mean CT values ranged from 22.28 to 22.65. The PCR products of Wnt4 and GAPDH were subcloned to TA cloning vector TM (Promega, Biotec, Madison, WI) as described previously (25). The plasmids containing Wnt4 cDNA and GAPDH cDNA were used to make standard curves of quantitative PCR.

Reporter Constructs

The cyclin D1 reporter construct used for the luciferase assays contained human cyclin D1 promoter from residues −944 to +139 cloned upstream of the luciferase gene (generous gift of Dr. M. Eilers) (29). Wnt-4 and β-catenin-dN (deletion of the amino-terminal region,

accumulated form) from human cDNAs were kindly provided by Dr. K. Matsumoto (30). The pCH110 reporter construct contained the SV40 promoter upstream of the β-galactosidase gene (Pharmacia Biotechnology Inc., Uppsala, Sweden).

Transient Transfection and Luciferase Assay

LLC-PK1 cells were transfected by the electroporation method. Plasmid DNAs (10 μg) were transfected by electroporation. Luciferase activity was measured 48 h after transfection. Data are representative of at least four independent experiments performed in duplicate and expressed as the "*n*-fold increase in luciferase activity" calculated relative to the indicated level of cyclin D1 promoter activity. Normalization was achieved by co-transfecting a β-galactosidase reporter construct as described previously (12). Luciferase and β-galactosidase activities were measured according to the Promega (Madison, WI) protocol.

Cell Cycle Analysis by [^{3}H]-Thymidine Incorporation and Flow Cytometry

After transfection, the LLC-PK1 cells were plated in 24-well plates and incubated in a medium without FCS for 20 h. For the last 4 h, the cells were pulsed with 1 μCi [^{3}H]-thymidine (Amersham). After the incubation, the cells were washed three times in ice-cold PBS, precipitated two times with 10% TCA, redissolved in 0.5 M NaOH, and counted in Aquasol-2 scintillation cocktail (NEN Research Products, Boston, MA).

LLC-PK1 cells were cultured in a 75-cm^2 flask. After transfection, the cells were incubated in a medium plus 10% FCS for 24 h, washed twice with PBS, and then resuspended in 70% ethanol for at least 12 h at 4°C. Fixed and permeabilized cells were collected by centrifugation and washed with PBS. The cells were stained with propidium iodide and analyzed by flow cytometry using a Coulter EPICS 753 flow cytometer to determine the percentages of the cells in the G1, S, and G2/M phases (31). All experiments were repeated at least four times.

Statistical Analyses

Results are given as means ± SD when comparing groups with equal sample numbers. Results are given as means ± SEM when comparing groups with different sample numbers. The differences were tested using two way-ANOVA followed by the Scheffe test for multiple comparisons. Two groups were compared by the unpaired *t* test. $P < 0.05$ was considered significant.

Results

Western Blot Analysis of the Protein Expressions of Wnt-4, Cyclin D1, and Cyclin A after Ischemic Renal Failure

The left renal artery was clamped for 60 min, and the left kidney was excised at 6, 12, 24, 48, and 72 h after reperfusion. Western blot analysis was used to detect the protein levels of Wnt-4, cyclin D1, and cyclin A. In an earlier study, Wnt-4 was reported to be expressed in the renal tubular cells of both embryonic and neonatal kidneys (32). For a positive control in our study, we used the neonatal rat kidney (Figure 1A), an organ that exhibits a clear positive signal. Weak expression of Wnt-4 was detected in the control adult kidney at 0 h (Figure 1, A and C). Wnt-4 dramatically increased at 6 to 12 h after ischemia/reperfusion (Figure 1C). The upregulation of Wnt-4 protein expression was temporary. The intensity of the Wnt-4 band declined at 24, 48, and 72 h after ischemia/reperfusion. We also examined the protein expressions of cyclin D1 and cyclin A. The band intensity of cyclin D1 was detectable in control (0 h) and at 6 and 12 h after ischemia/reperfusion and increased at 24 h after ischemia/reperfusion (Figure 1E). The band intensity of cyclin A was very weak in control (0 h), as well as in the ischemia/reperfusion kidneys at 6 and 12 h. At 24 to 48 h after ischemia/reperfusion, the expression of cyclin A increased (Figure 1G).

Immunohistochemical Examination of Wnt-4 in ARF

We next performed immunohistologic studies on Wnt-4 using confocal microscopy (Figures 2 and 3). In the lower-power view, Wnt-4 expression was observed in cortical renal tubules at 12 h after ischemia/reperfusion. (Figure 2A). Anti-aquaporin-1 antibody was used as a marker of proximal tubules (21–23). The expression of Wnt-4 was apparently co-localized with aquaporin-1 in the lower-power view (Figure 2, B and C) but undetectable in the renal cortices from the control rats (Figure 2G). The expression of aquaporin-1 was clearly observed in renal cortices from the control rats (Figure 2H). Taken together, these results demonstrate a prevalence of Wnt-4 expression in the proximal tubules of the renal cortex 12 h after ischemia/reperfusion (Figsure 2, A through C). Wnt-4 was undetectable in the renal medullae of both the ischemia/reperfusion kidneys and control kidneys (Figure 2, D and J). Only minimal staining of aquaporin-1 was observed in the medullae of the ischemia/reperfusion and control kidneys (Figure 2, E and K). In the higher-power view, Wnt-4 staining was observed in intracellular location of proximal tubular cells (Figure 3A). In double-staining, these cells were stained positively by aquaporin-1 antibody (Figure 3, B and C). When blocking peptide was added to the anti-Wnt-4 antibody solution, no positive signal was observed (Figure 3D)

To examine the intracellular localization of Wnt-4 in renal tubules, we performed immunohistochemical studies on the colocalization using anti-Wnt-4 and anti-GM130 antibodies. The anti-GM130 antibody was used as a Golgi apparatus marker (20). Wnt-4 staining was observed intracellularly at locations (Figure 4, A and D) overlapping the areas stained by GM130 (Figure 4, B and E). In the double-staining of Wnt-4 and GM130, the Wnt-4 staining appeared in the Golgi apparatus (yellow staining in Figure 4, C and F).

To colocalize Wnt-4 with dividing cells, a lower-power view of Wnt-4 staining and PCNA staining was examined at 24 h after ischemia/reperfusion (Figure 5). Wnt-4 staining and PCNA staining were both observed at the proximal tubules of the cortex (Figures 5, A, B, and C). In the higher-power view of Wnt-4 staining, Wnt-4 and PCNA were co-localized in the same tubular cells at 24 h after ischemia/reperfusion (Figure 5, D, E, and F).

Real-Time PCR

Quantitation of Wnt-4 mRNA transcript using the real-time quantitative PCR method revealed 6.5-fold (3 h), 15.2-fold (6 h), 8.1-fold (12 h), and 3.7-fold (24 h) increases in Wnt-4 mRNA levels, compared with the 0 h value (Figure 6A). With

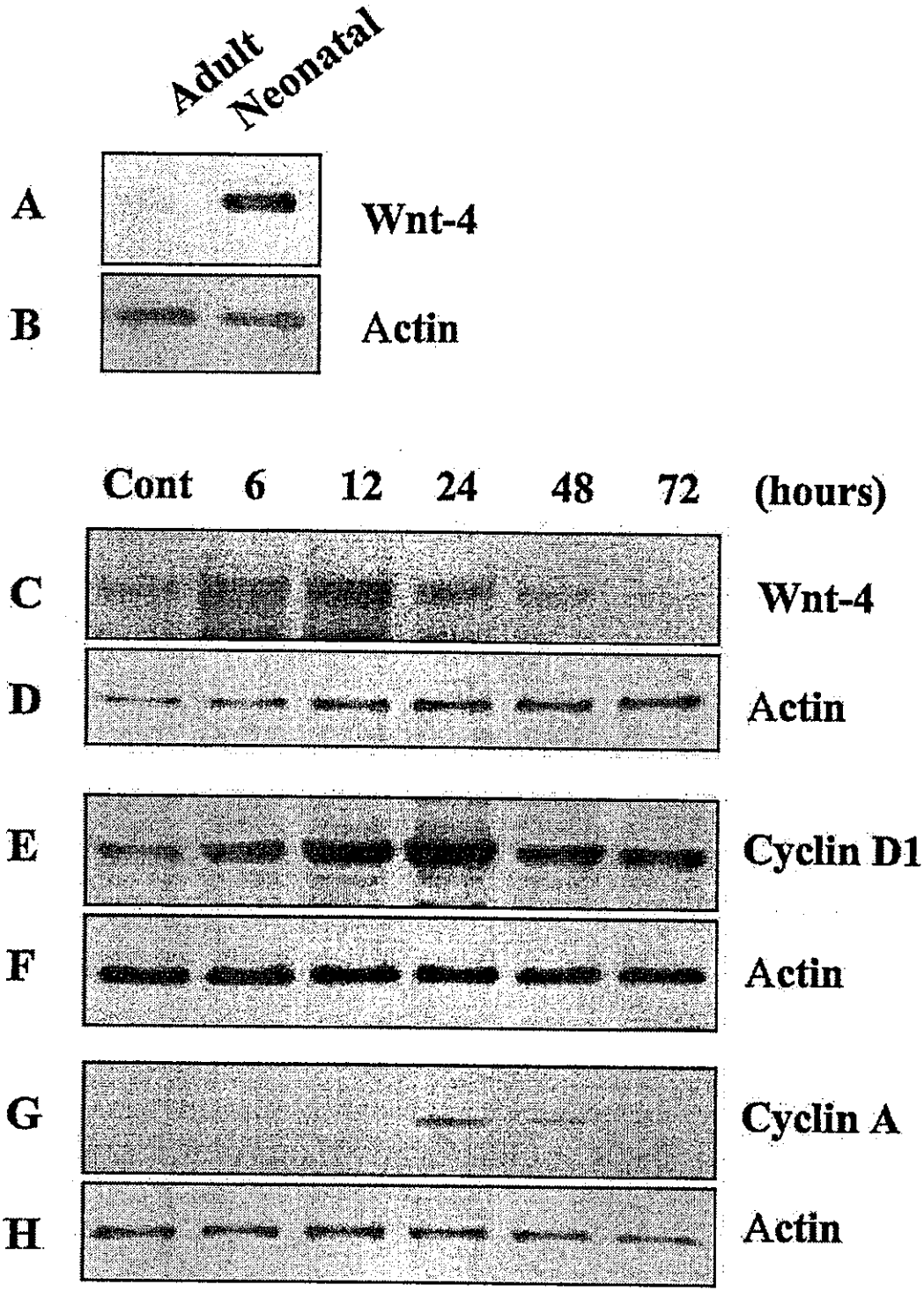

Figure 1. Protein expressions of Wnt-4, cyclin D1, and cyclin A in the kidneys of rats subjected to 60 min of renal ischemia. Bilateral renal arteries were clamped for 60 min, and kidneys were excised at 6, 12, 24, 48, and 72 h after reperfusion. Rats that received sham operations at 0 h served as controls. In the case of Wnt-4, neonatal rat renal protein (20 μg) was loaded as a positive control (right lane) (A). Extracted protein (20 μg) from renal tissue was separated by SDS-PAGE gels. Wnt-4, cyclin D1, and cyclin A protein levels were detected by Western blot analysis (C, F, G). Western blots of actin as loading controls are shown (B, D, F, H). Three membranes were used for panels C through H: the first for panels C (Wnt-4) and D (actin), the second for panels E (cyclin D1) and F (actin), and the third for panels G (cyclin A) and H (actin). These three membranes were equally loaded of the renal protein.

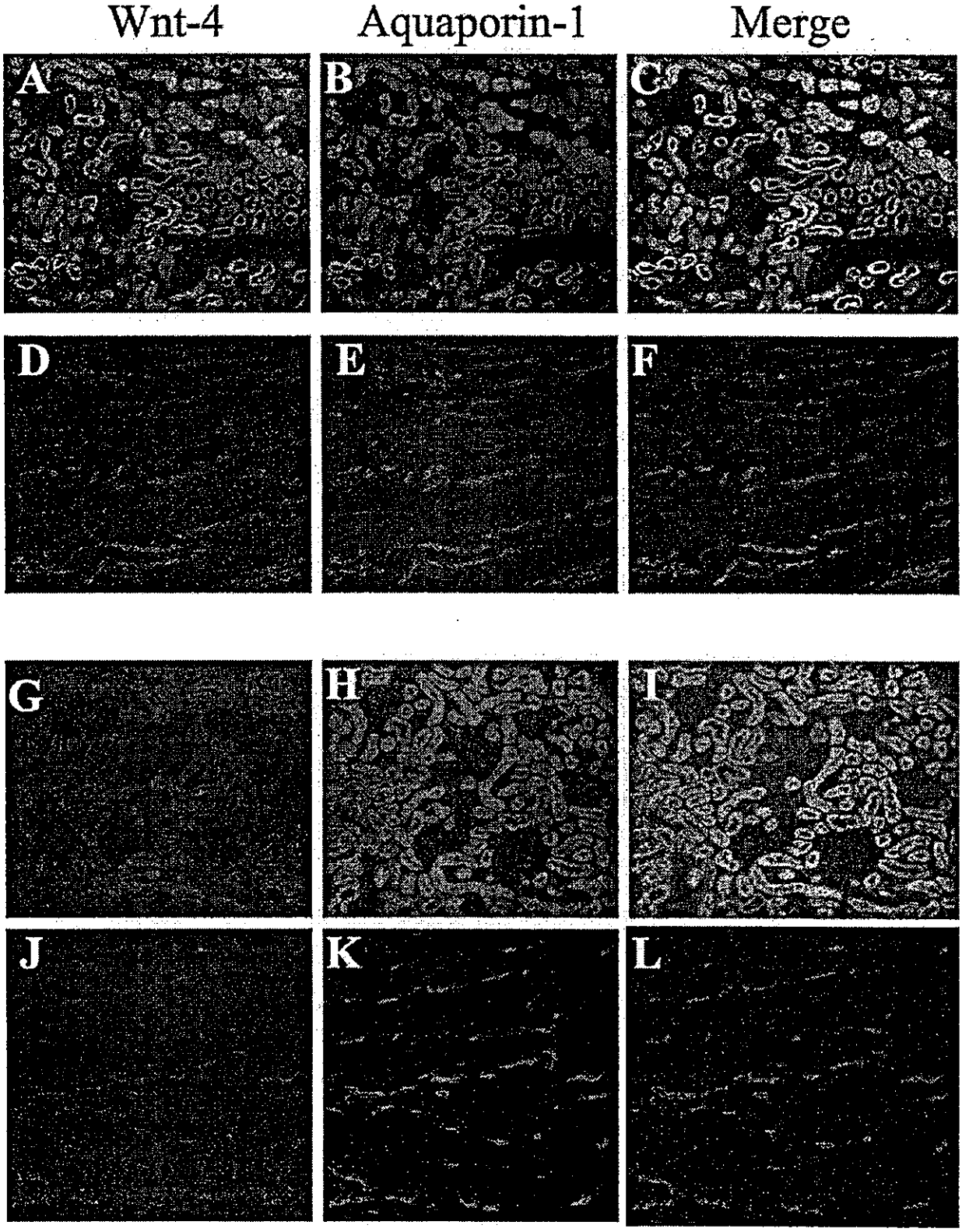

Figure 2. Immunohistologic examination of Wnt-4 in ischemic-reperfusion kidneys and control kidneys. Immunohistochemical analyses of lower-power views (×100) of the renal cortex were performed with antibody against Wnt-4 (A), antibody against aquaporin-1 (B), and in a merged condition (C) at 12 h after ischemic injury. Immunohistochemical analyses of lower-power views (×100) of the renal medulla were performed with antibody against Wnt-4 (D), antibody against aquaporin-1 (E), and in a merged condition (F) at 12 h after ischemic injury. Immunohistochemical analyses of the lower-power view (×100) of the renal cortex were performed with antibody against Wnt-4 (G), antibody against aquaporin-1 (H), and in a merged condition (I) at the control kidney. Immunohistochemical analyses of lower-power views (×100) of the renal medulla were performed with antibody against Wnt-4 (J), antibody against aquaporin-1 (K), and in a merged condition (L) at the control kidney.

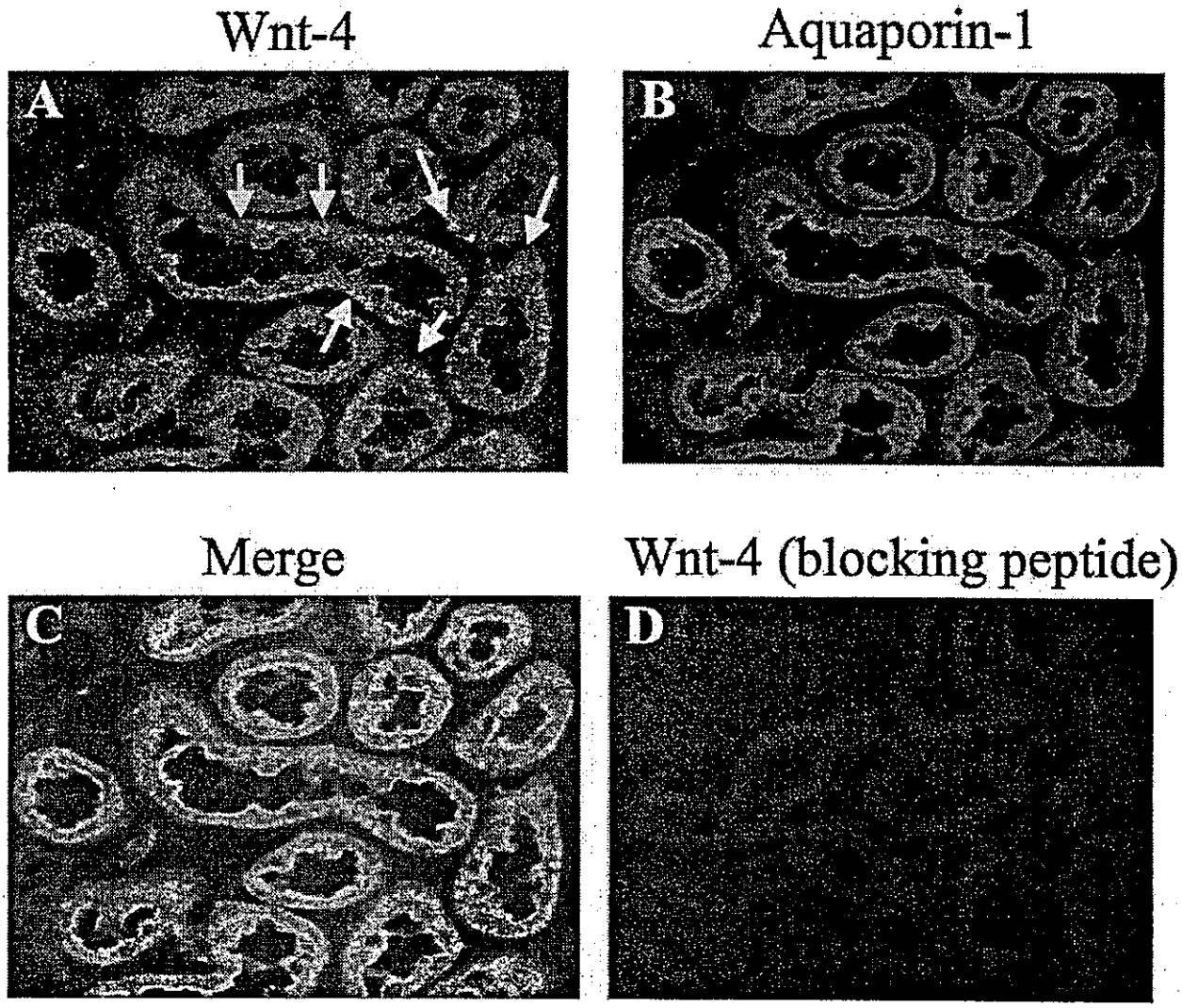

Figure 3. Immunohistologic examination of Wnt-4 in proximal tubules of ischemic-reperfusion kidneys. Immunohistochemical analyses of higher-power views (×400) of the renal cortex were performed with antibody against Wnt-4 (A), antibody against aquaporin-1 (B), and in a merged condition (C) at 12 h after ischemic injury. When blocking peptide was added to the anti-Wnt-4 antibody solution, no positive signal was observed (D). The arrows indicate Wnt-4–positive cells.

the use of the Wnt-4 and GAPDH cDNA plasmids, the linear curve between the PCR product and quantity of cDNA (10 pg/μl to 100 ng/μl) was observed in the utilized range. Wnt-4 mRNA expression was also significantly upregulated in neonatal kidney (Figure 6B). GAPDH signal was not significantly changed by ischemia/reperfusion (Figure 6C).

Cell Cycle Progression by Overexpression of Wnt-4 in LLC-PK1 Cells

Initially, we examined how the Wnt-4-β-catenin pathway affected the proliferation of LLC-PK1 cells by [^{3}H]-thymidine uptake. Figure 7A shows the effects of the Wnt-4-β-catenin pathway on [^{3}H]-thymidine uptake. Transfection of Wnt-4, β-catenin dN, and co-transfection of Wnt-4 and β-catenin dN stimulated the [^{3}H]-thymidine uptake to 186, 137, and 225%, respectively. We next used flow cytometry to examine the effects of the Wnt-4-β-catenin pathway on cell cycle progression. When LLC-PK1 cells expressing Wnt-4 and β-catenin were incubated without FCS for 24 h, the percentages of S and G2/M phases were increased from 15.5% to 23.5% and from 30.5% to 47.3%, respectively, compared with the levels in the cells transfected with empty vector (Figure 7, B and C). These results demonstrated the stimulatory effects of the Wnt-4 and β-catenin pathways on cell cycle progression.

Stimulation of Cyclin D1 Promoter Activities by Overexpression of Wnt-4 and β-Catenin

We next examined the role of the Wnt-4-β-catenin signaling pathway in the regulation of cyclin D1 promoter activity and protein expression. We performed a transient transfection with

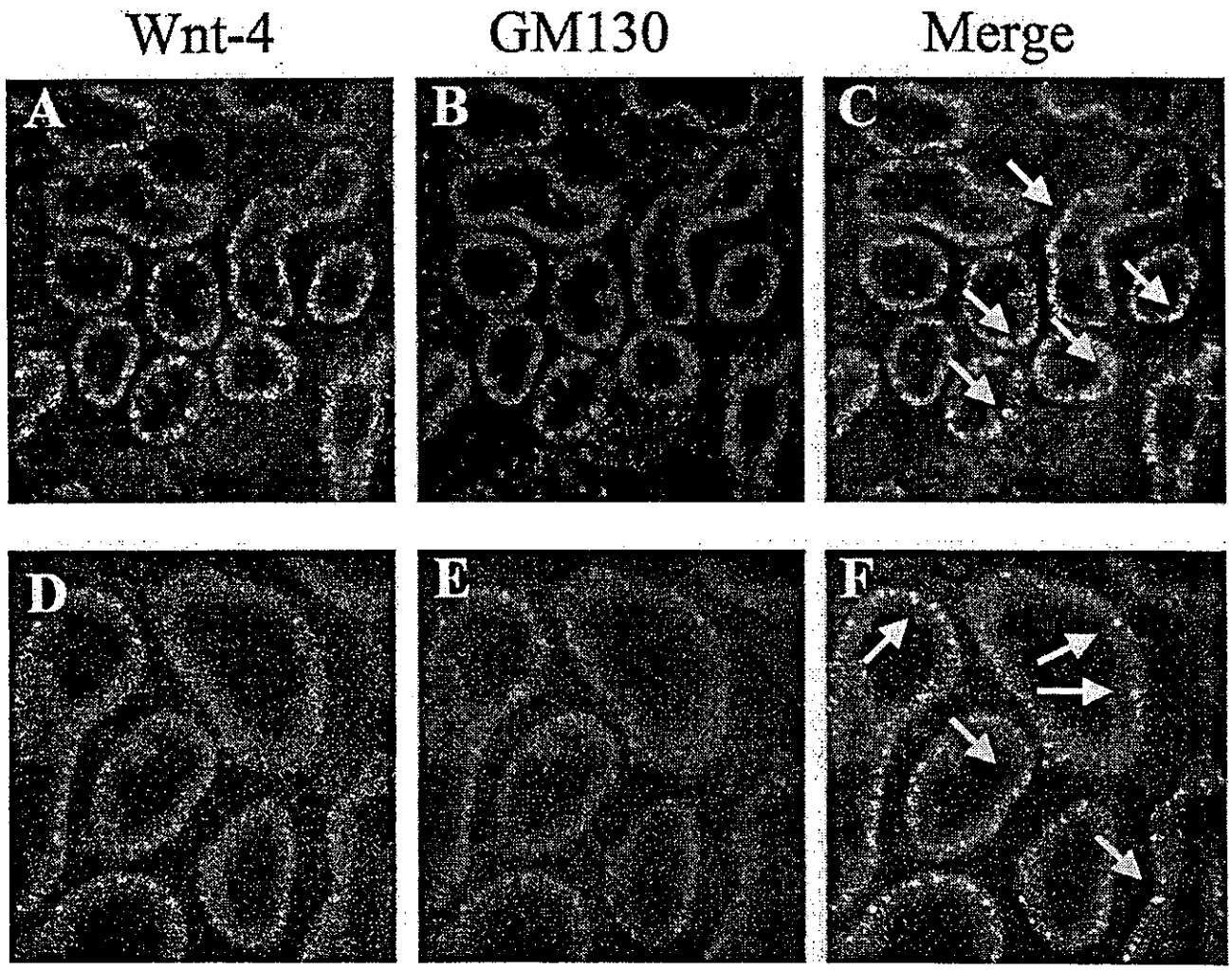

Figure 4. Immunohistologic colocalization of Wnt-4 and GM130 in proximal tubules of ischemic-reperfusion kidneys. Immunohistochemical analyses of high-power views (×400) of the renal cortex were performed with antibody against Wnt-4 (A), antibody against GM130 (B), and in a merged condition (C) at 12 h after ischemic injury. Immunohistochemical analyses of higher-power views (×650) of the renal cortex were performed with antibody against Wnt-4 (D), antibody against GM130 (E), and in a merged condition (F) at 12 h after ischemic injury. The arrows indicate Wnt-4–positive and GM130–positive cells.

either an empty vector or vector containing Wnt-4 and β-catenin dN, together with the cyclin D1-luciferase reporter gene and β-galactosidase expression vector. When Wnt-4, β-catenin dN, and Wnt-4-β-catenin dN were expressed in LLC-PK1 cells cultured in a DMEM medium without FCS, cyclin D1 promoter activity increased significantly to 2.5-, 2.8-, and 4.8-fold their control levels, respectively (Figure 8A). We further examined the regulation of cyclin D1 protein expression when Wnt-4 and β-catenin dN plasmids were co-transfected. When Wnt-4 and β-catenin dN plasmids were transfected, the cells expressed higher levels of cyclin D1 than the cells transfected with the empty vector (Figure 8B). This result suggested that the Wnt-4-β-catenin pathway positively regulates cyclin D1 promoter activity and protein expression in renal tubular cells.

Discussion

In the present study, we demonstrate (*1*) that Wnt-4 is upregulated in the proximal tubules during recovery from ARF and (*2*) that Wnt-4 expression is localized in the Golgi apparatus and co-localized with PCNA in the renal tubules during ARF. Our findings additionally suggest that the Wnt-4-β-catenin pathway may regulate the transcription of cyclin D1 and cell cycle progression in the renal tubules during ARF.

Recovery from ARF requires the replacement of damaged cells with new cells that restore tubule epithelial integrity. Regeneration processes are characterized by proliferation of dedifferentiated cells and subsequent redifferentiation of the daughter cells into the required cell phenotypes. Noting the similarity between this process and the cellular phenomena observed during embryogenesis, investigators have postulated

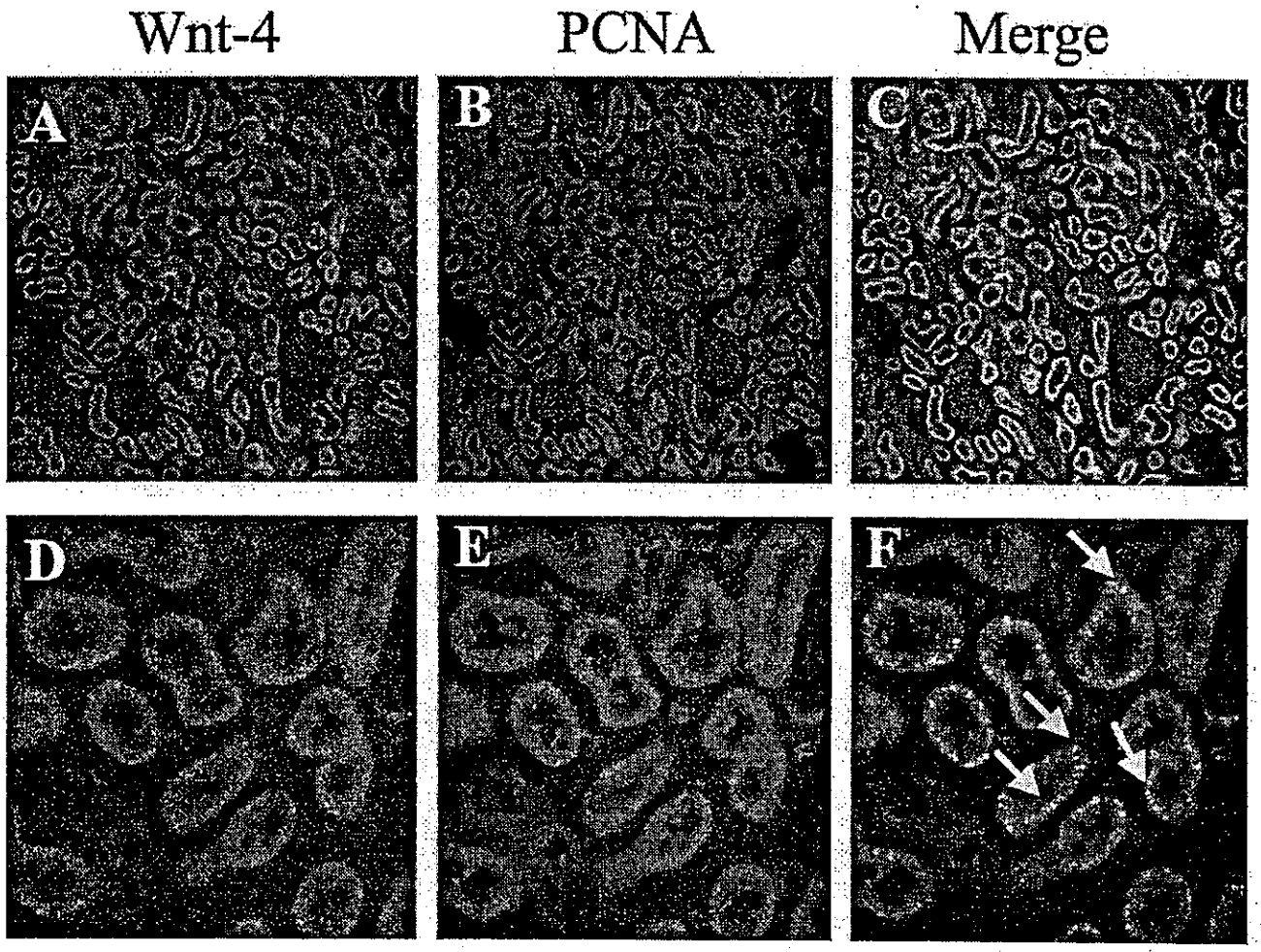

Figure 5. Immunohistologic colocalization of Wnt-4 and PCNA in proximal tubules of ischemic-reperfusion kidneys. Immunohistochemical analyses of lower-power views (×100) of the renal cortex were performed with antibody against Wnt-4 (A), antibody against PCNA (B), and in a merged condition (C) at 24 h after ischemic injury. Immunohistochemical analyses of higher-power views (×400) of the renal cortex were performed with antibody against Wnt-4 (D), antibody against PCNA (E), and in a merged condition (F) at 24 h after ischemic injury. The arrows indicate Wnt-4–positive and PCNA–positive cells.

that regeneration processes to reestablish proper tissue function after damage may repeat parts of the genetic program that serve during organogenesis (5,33). To test this hypothesis, we examined the patterns of Wnt-4 expression in a model of acute renal ischemia.

Our study is the first to demonstrate that Wnt-4 expression is upregulated in the early phase of ischemic acute renal failure. Wnt-4 expression in the proximal tubule was localized exclusively to the site of tubule regeneration, where PCNA is also expressed. Accordingly, we speculated that Wnt-4 protein may induce the transformation of regenerative renal tubular cells. In the developmental stage, Wnt-4 is expressed in pretubular aggregates of the condensing mesenchyme during development to the comma- and S-shaped bodies of metanephric kidneys (15). Thus, our data suggested that the cells that express Wnt-4 after ischemic injury have characteristics of embryonic renal cells such as mesenchymal-to-epithelial progression and proliferation. The origin of the Wnt-4-positive cells is an interesting issue. At least two possible origins can be considered: the primitive cells relining the outer medullary portion of the proximal tubule, and the differentiated surviving cells of the superficial cortex. We are inclined to believe the latter possibility, given the presentation of the Wnt-4–positive cells mainly in the cortex, as shown in Figure 2A. These findings suggest that the differentiated surviving cells of the cortical tubules may express Wnt-4 after ischemic injury.

In a study on the expression of the Wnt gene family (Wnt-4, -7b, and -11) during late nephrogenesis and complete ureteral obstruction, Nguyen *et al.* (32) found that Wnt-4 and Wnt-11 were important mediators of the transformation of mesenchyme to epithelium in the kidney. It thus seems that other members of the Wnt family may work together with Wnt-4 in regenerating the renal tubules after ischemic ARF. Further studies may be necessary to clarify these issues.

Surendran *et al.* (34) recently observed low levels of Wnt-4 mRNA in the normal adult mouse kidney and that high levels

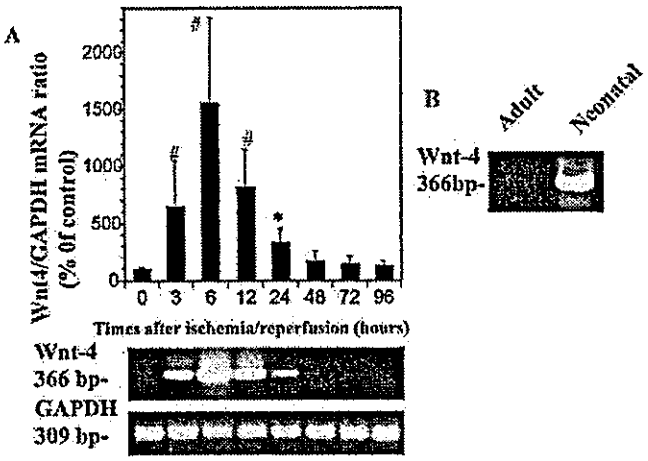

Figure 6. Quantitative analysis of Wnt-4 expression in ischemic-reperfusion kidneys using real-time PCR. (A) Bilateral renal arteries were clamped for 60 min, and kidneys were excised at 3, 6, 12, 24, 48, 72, and 96 h after reperfusion. Sham-operated rats at 0 h served as controls. Extracted total RNAs were subjected to quantitative PCR using the LightCycler Real-time PCR for the estimation of relative Wnt-4 mRNA levels and the ratio of Wnt-4 to GAPDH mRNA, as described in the Materials and Methods section. Each column with a bar shows the mean ± SD ($n = 5$). * $P < 0.05$, # $P < 0.001$ *versus* control rats. The representative agarose gels for Wnt-4 and GAPDH are shown (lower figures). (B) Extracted total RNAs from control adult kidney and neonatal rat kidney were subjected to RT-PCR.

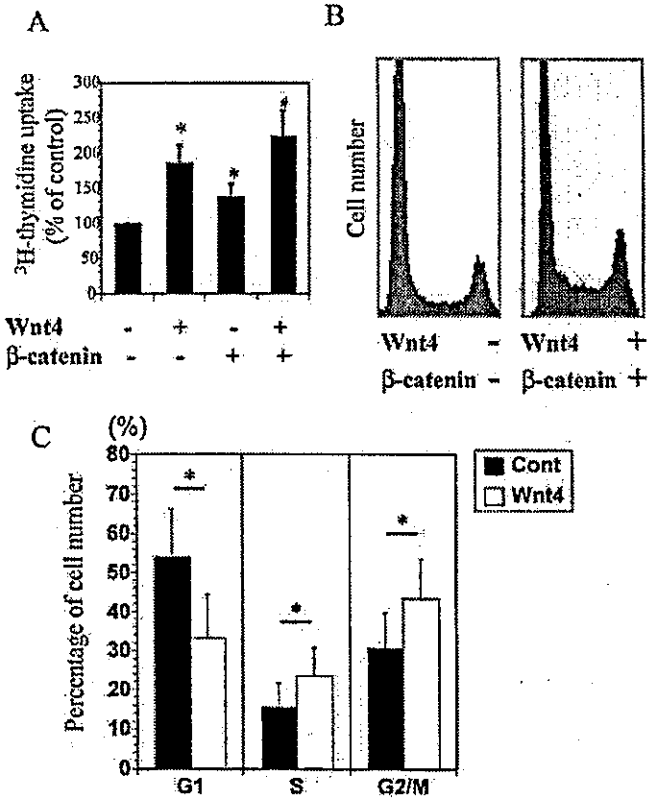

Figure 7. Regulation of renal tubular cell proliferation by overexpression of Wnt-4 and β-catenin. (A) The cells were transfected with plasmids containing Wnt-4, β-catenin dN, or pCDNA3 (vector) and incubated with DMEM medium without FCS for 24 h. [^{3}H]-thymidine incorporation was measured during the last 4 h. Results are means ± SEM of five or six independent experiments. * $P < 0.05$; # $P < 0.01$. (B) LLC-PK1 cells expressing pCDNA3 (empty vector) or Wnt-4 and β-catenin dN were incubated in DMEM medium with or without FCS for 24 h. The percentages of S phase and G2/M phase were analyzed by flow cytometry using a FACS flow cytometer. Cell cycle analyses by flow cytometry were performed four times. (C) The percentages of G1 phase, S phase, and G2/M phase were analyzed. Each bar represents the mean ± SD; $n = 4$; *$P < 0.05$ by ANOVA.

of Wnt-4 expression induced in the collecting ducts in murine models of renal injury that produced tubulointerstitial fibrosis. In the ischemia/reperfusion model in our study, we did not observe a fibrotic area in the proximal tubules. It will be of interest to examine whether Wnt-4 plays a role in fibrogenesis in renal tubular cells.

Our data are also the first to demonstrate the contribution of Wnt-4-β-catenin signaling to the activation of cyclin D1 and promoter and protein expression in renal tubular cells. The Wnt-β-catenin pathway plays a key role in normal embryonic development and in malignant transformation of many types of human cells (13). Recent reports indicate that β-catenin activates transcription from the cyclin D1 promoter and also that sequences within the promoter related to consensus TCF/LEF-binding sites are necessary for activation in colon carcinoma cells (19). However, the functional role of the Wnt-4/β-catenin signaling pathway in non-carcinoma cells is not known well. Our data demonstrate that overexpression of Wnt-4 increases cyclin D1 promoter activity and protein expression in non-carcinoma, renal epithelial cells. Moreover, the co-expression of β-catenin further increased the promoter activity and protein expression of cyclin D1. These data suggest that the Wnt-4 protein might activate a cascade of signaling events that leads to an increase in the intracellular availability of β-catenin in renal tubular cells. Within the nucleus, β-catenin interacts with the TCF family and regulates gene expression via the TCF binding site (13,16). Our data suggest that the overexpression of Wnt-4 and β-catenin induce cell cycle progression in renal tubular cells. If this is the case, then the expression of Wnt-4 in the recovery phase of ARF could be expected to promote cell cycle progression after tubular injury. While we lack clear evidence that Wnt-4 is a proliferative signal during tubulogenesis, our data demonstrate that *in vitro* Wnt-4 and β-catenin proliferate renal tubular cells. Wnt-4 has been proven to be required for metanephric condensation during development, and there is no evidence suggesting that Wnt-4 is a proliferative signal in metanephric formation. In our ischemia/reperfusion model, Wnt-4 was co-localized with PCNA, suggesting that Wnt-4 might be proliferative signal in regenerating renal tubules. Dysregulated activation of Wnt-4 and β-catenin pathways has been reported in malignancies such as colon carcinoma cells and melanoma. The transient but less than persistent expression may prevent renal tubular cells from becoming hyperplastic or malignant.